ELSEVIER

Contents lists available at ScienceDirect

Journal of Power Sources

journal homepage: www.elsevier.com/locate/jpowsour





Mechanistic understanding of Li dendrites growth by *in-situ/operando* imaging techniques

Tara Foroozan, Soroosh Sharifi-Asl, Reza Shahbazian-Yassar

Mechanical and Industrial Engineering Department, University of Illinois at Chicago, Chicago, IL, 60607, United States

HIGHLIGHTS

- •In-situ and operando imaging techniques for studying lithium dendrite growth.
- •Optical, electron, scanning probe, X-ray, neutron and resonance-based imaging.
- •Visualization of the Li-dendrite nucleation and growth.
- •In-depth understanding of Li dendrite formation mechanism.
- •Outlook and future directions of in-situ imaging techniques for Li dendrite studies.

ARTICLE INFO

Keywords: In-situ imaging Operando imaging Li dendrite formation Li-metal anode

ABSTRACT

Lithium (Li) metal is the holy grail of anode materials for high energy density batteries. However, safety hazards due to the formation of Li dendrites have prevented their commercialization. This study provides a comprehensive review of the recent works on the mechanisms of Li dendrite formation utilizing *in-situ* and *operando* imaging techniques. These multiscale and multimodal techniques include optical imaging, electron microscopy, scanning probe microscopy, X-ray imaging, neutron microscopy and resonance-based imaging techniques. Briefly, optical microscopy enables visualization of Li morphological transitions, and if coupled with a Raman spectrometer, can provide chemical imaging of the Li/electrolyte interface. Electron microscopy and scanning probe imaging offer high spatial resolution enabling near-atomic structural studies of Li dendrites and solid electrolyte interphases. X-ray based techniques offer a high beam penetration depth allowing the study of Li microstructure evolution in large cells. Neutron imaging based on ⁶Li has higher sensitivity compared to X-ray imaging and can visualize the Li-ion concentration as a function of sample depth, while ⁷Li nuclear magnetic resonance allows for quantified analysis of Li microstructures and provide chemical and spatial information on Li microstructural growth. Finally, some prospective directions for further utilization of *in-situ/operando* imaging techniques in Li anode research was proposed.

1. Introduction

Since 1970s, lithium (Li) metal has been known to be the holy grail of electrode materials, due to its large theoretical capacity (3860 mAh g $^{-1}$) and low redox potential (-3.04~V vs standard hydrogen potential, $H_2/$ H^+) [1]. In 1971, Exxon demonstrated the practical application of Li metal batteries in digital watches, calculators, and implantable medical devices, where Li metal was used as anode and titanium sulfide (TiS2) as cathode [2]. However, Li metal batteries showed poor cycle stability and safety hazards, which prevented their commercial application [3]. These issues stem from the high reactivity of Li, instability of the Li

metal/electrolyte interface, hostless nature of Li metal and its natural dendritic electrodeposition [4]. Brissot et al. [5] showed that the dendritic Li microstructures can reach the positive electrode, causing internal short circuit leading to fast discharge, heating and eventually explosion of the cell. The associated problems rendered lithium metal batteries (LMBs) to lose the opportunity of the commercial market. Consequently, research on LMBs slowed down and the focus was placed on finding alternative materials to replace lithium. As a result, the rechargeable Li-ion batteries (LIBs) based on graphite anode were invented, which have revolutionized many applications ranging from consumer electronics to electric transportation [6]. However, direct

E-mail address: rsyassar@uic.edu (R. Shahbazian-Yassar).

^{*} Corresponding author.

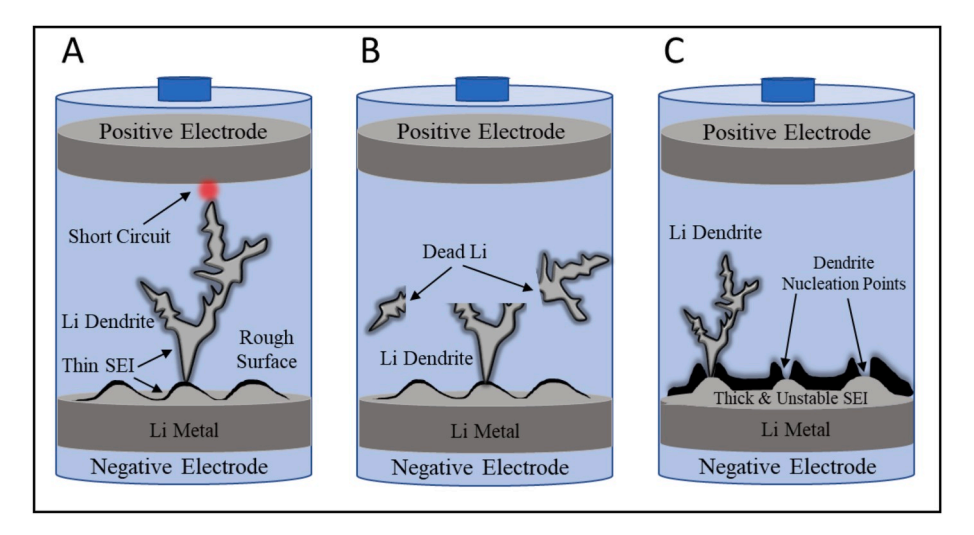


Fig. 1. Representative schematic of the main challenges associated with Li metal anode: (a) short circuit induced by Li dendrites, (b) formation of inactive (dead) Li, and (c) development of thick and mechanically unstable SEI.

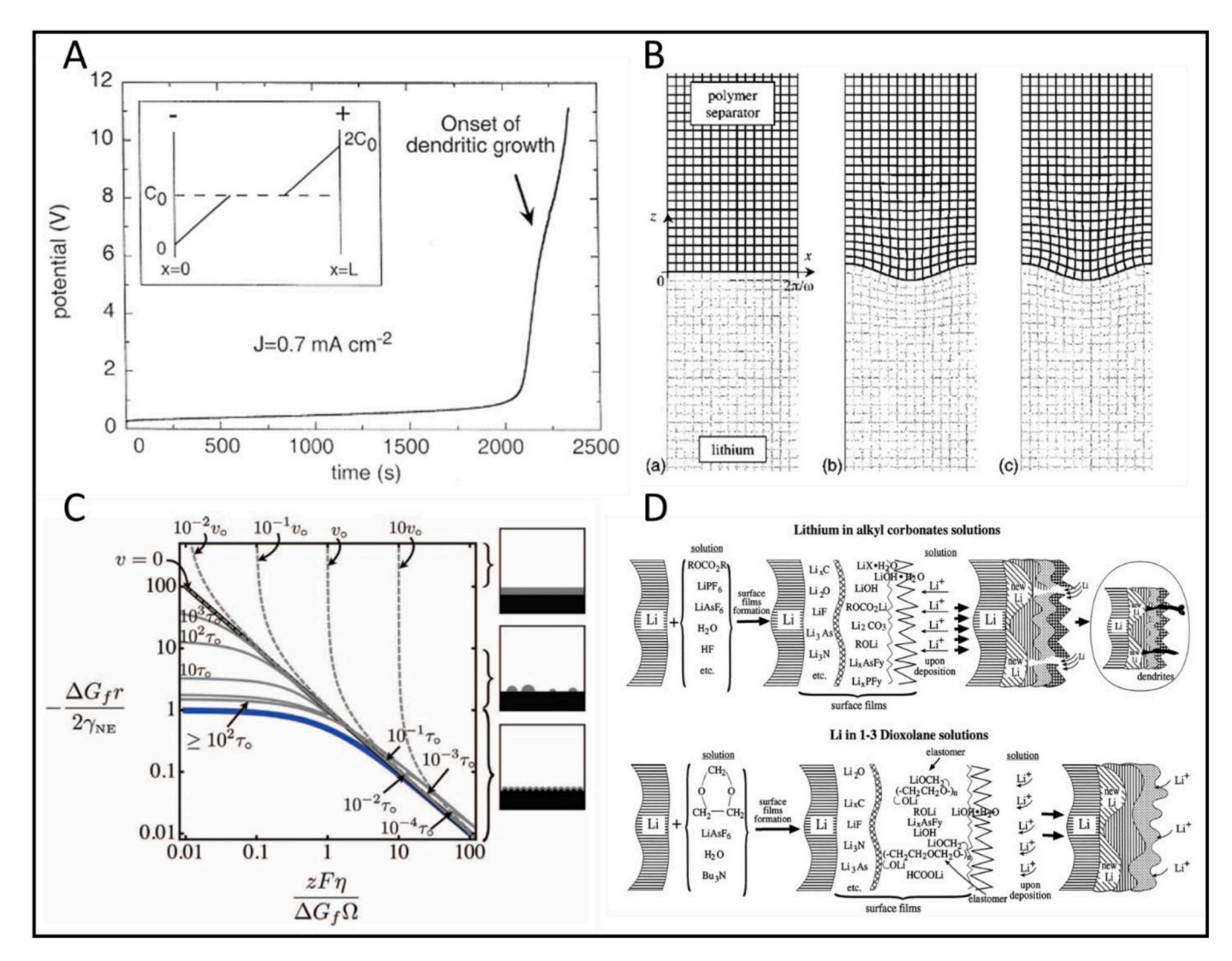


Fig. 2. Widely accepted parameters affecting the Li dendrite growth: (a) ionic concentration gradient and growth of dendrite at Sand's time: Reproduced with permission [16]. Copyright 1990, American Physical Society, (b) effect of separator's mechanical stability of the roughness of Li interface: Reproduced with permission [20]. Copyright 2005, Electrochemical Society, (c) effect of surface tension and overpotential driving forces in the Li dendrite growth mode: Reproduced with permission [27]. Copyright 2013, Electrochemical Society, (d) SEI contribution to the formation of Li dendrites: Reproduced with permission [31]. Copyright 2000, Elsevier.

incorporation of Li metal as the anode has remained the ultimate goal of battery community, as Li metal can provide 10 times the capacity of currently utilized graphite anodes. To achieve this target, extensive studies are underway to understand the dendritic Li deposition as the key parameter determining the safety and life cycle of Li-metal batteries.

Overall, the Li-metal challenges can be summarized to be due to the (1) dendritic electrodeposition of Li metal (Fig. 1A), (2) formation of inactive Li (Fig. 1B), and (3) development of thick and mechanically unstable solid electrolyte interface (SEI) (Fig. 1C), all of which occur at the interface between Li metal electrode and electrolyte. It is suggested that Li dendrites form around the protuberances of the electrode surface with enhanced electric field [7-10]. Meanwhile, the SEI spontaneously formed at the interface of Li and electrolyte is not mechanically stable enough to accommodate the high volume changes of the Li anode during repeated Li deposition/dissolution leading to the localized formation of Li dendrites and excess consumption of fresh Li and electrolyte [11,12]. In addition, during prolonged cycling, the Li dendrites with narrow roots can easily detach from the electrically conducting deposition substrate and form electrochemically inactive (dead) Li. Under extreme circumstances, Li dendrites can make internal short circuit between the electrodes and cause catastrophic phenomena and explosion of the cell [13, 14]. Below we briefly discuss the highly accepted models for the growth of Li dendrites that are mainly related to ion transport, surface reactions and mechanical stabilities at the interface of lithium and electrolyte. Then, we discuss the crucial role of in-situ/operando imaging techniques for in-depth understanding of Li dendrite growth mechanism and elaborate on the recent advancements in this field. Challenges associated with in-situ/operando imaging techniques, and potential new contributions of these techniques to gain more in-depth understanding of Li dendrites are also discussed.

2. Understanding Li dendrites formation and growth

To investigate the deposition behavior of metallic Li at the nucleation and early stages of dendrite growth, many groups have modeled the Li dendrite formation and growth process. Chazalviel's electromigration-limited (space charge) model and its derived ones have been widely accepted for decades to be responsible for the Li dendrites growth [15]. According to this model, under polarization, the electrolyte moves away from the steady-state ionic concentration, where Li+ ions and anions diverge and move towards the negative and positive electrodes, respectively. Under this condition, Li⁺ ions obtain electron from the electrode surface and are reduced to Li. At the macroscopic scale, constant supply of Li⁺ ions under the electric field compensates for the depletion of Li⁺ ions. However, this is not the case at microscopic scale and can greatly affect the deposition morphology of Li. Based on this understanding, Chazalviel et al. [5] described the Li dendrite growth by calculating the concentration gradient in a Li symmetric cell under operation $\left(\frac{\partial C}{\partial x}\left(x\right) = \frac{J \; \mu_a}{eD(\mu_a + \mu_{Ll^+})}\right)$. In this model, C is ionic concentration, xis the distance from the electrode surface, J is effective current density, D is diffusion coefficient, e is electronic charge and μ_a and μ_{Li}^+ are the anionic and Li⁺ mobility, respectively. Based on Chazalviel's electromigration-limited model, with the inter-electrode distance L and initial Li salt concentration C_0 , if $dC/dx > 2C_0/L$, the ionic concentration at the negative electrode surface goes to zero. So at high current densities, exceeding diffusion limitation, the violation of neutrality near the electrode surface can form a space charge in dilute solutions and at a specific time defined as "Sand's time" ($T = \pi D \left(\frac{eC_0}{2\hbar t_a}\right)^2$, the scarce supply

of Li cations preferentially deposits onto surface protuberances forming Li dendrites (i.e. tip growth mode) (Fig. 2A) [16]. T is Sand's time, C_0 is the initial concentration where t_a is the anionic transference as $1-t_{Li}^+$ $=\frac{\mu_a}{\mu_a+\mu_{Li}}$. Based on their model, at low effective current density where $dC/dx < 2C_0/L$, a stable ionic concentration gradient exists, and no Li

dendrites will form. However, Rosso et al. [17] observed Li dendrites at lower current densities predicted by Chazalviel. Rosso et al. [17] and Teyssot et al. [18] proposed that the Chazalviel's model can be extended to low currents due to the nanoscale inhomogeneity in concentration around surface protuberances. Based on these understandings, Li deposition occurs readily on the surface protrusions due to the higher effective current density and lower Sand's time, leading to tip-induced nucleation of dendrites. Chazalviel's model successfully explained the distribution of ionic concentration at the electrode tips and predicted that dendrite growth velocity, ν , is proportional to the applied electric field (E_0) and the mobility of the anions ($\nu = -\mu_a E_0$). However, *in-situ* imaging techniques have shown that other modes of root induced, and also multidirectional induced nucleation are also possible for Li electrodeposition, which we will discuss through this paper.

In contrast to the Chazalviel's model, Monroe and Newman [19] suggested a theory of dendrite growth based on the elasticity of the separator and discussed how shear modulus and Poisson's ratio of polymer electrolytes can affect roughness on the Li interface (Fig. 2B). They suggested that the dendrite growth is a tip surface-energy controlled reaction and is directly proportional to the overpotential and inversely proportional to the tip curvature of needle-like dendrites. They theoretically suggested the "double shear modulus theory", in which Li dendrites are expected to be mechanically suppressed when the shear modulus of the separator is about twice that of lithium ($\sim 10^9$ Pa) [20]. However, later on, it was experimentally shown that Li dendrites can penetrate even through the solid electrolytes with much larger shear modulus than what the Monroe and Newman model has predicated [21-23]. Experimental works suggest that other parameters such as defects, grain boundaries, and non-homogeneities in the interface are also responsible [24]. Furthermore, it was recently shown that mechanical strength of narrow Li dendrites is much higher than that of bulk Li, which can lead to easy penetration of Li dendrites through stiff structures like solid electrolytes and causing short circuit [25,26].

Ely and García [27] utilized the thermodynamic and kinetic analytical frameworks and incorporated the effect of surface tension and overpotential driving forces in the Li dendrite growth model. They proposed that an overpotential-controlled critical radius must be overcame before the dendrite formation begins. They suggested this mechanism for the reaction rate limited systems at low current densities. In the early stages of growth, they identified five regimes of behavior: nucleation suppression regime, long incubation time regime, short incubation time regime, early growth regime, and late growth regime. Below the blue curve in Fig. 2C is the nucleation suppression regime, where embryo sizes are not in favor of growth. Above the black curve is the growth regime, in which the nuclei sizes and overpotentials lead to stable growth of the electrodeposit. The long incubation time regime is above the blue curve and below the gray curve where stability of nuclei is dependent on the local fluctuations to reach the growth regime. They showed that dendrites start to grow after thermal fluctuations made stable growth kinetically favorable. Once the stable Li nuclei are established, evolution of the deposits will be dominated by the surface inhomogeneities and localized electric fields.

These models have established a foundation for understanding the nucleation and growth mechanisms of dendrites; however, they still have many limitations and can be highly simplified, which excels the importance of experimental contributions in understanding the details of Li dendrite growth. One critical factor in the dendritic growth of Li, which was not initially considered in theoretical simulations is the solid electrolyte interphase (SEI). The highly negative electrochemical potential of Li, besides delivering a very high energy density in LMBs, can lead to unavoidable surface reactions between Li, electrons and solvent species. In 1979, Peled realized the formation of a thin film at the interface of Li and electrolyte and named it solid electrolyte interphase (SEI) [28]. As discussed by Goodenough, considering the electrochemical stability window of the electrolyte components (the highest occupied molecular orbital (HOMO) and lowest unoccupied molecular

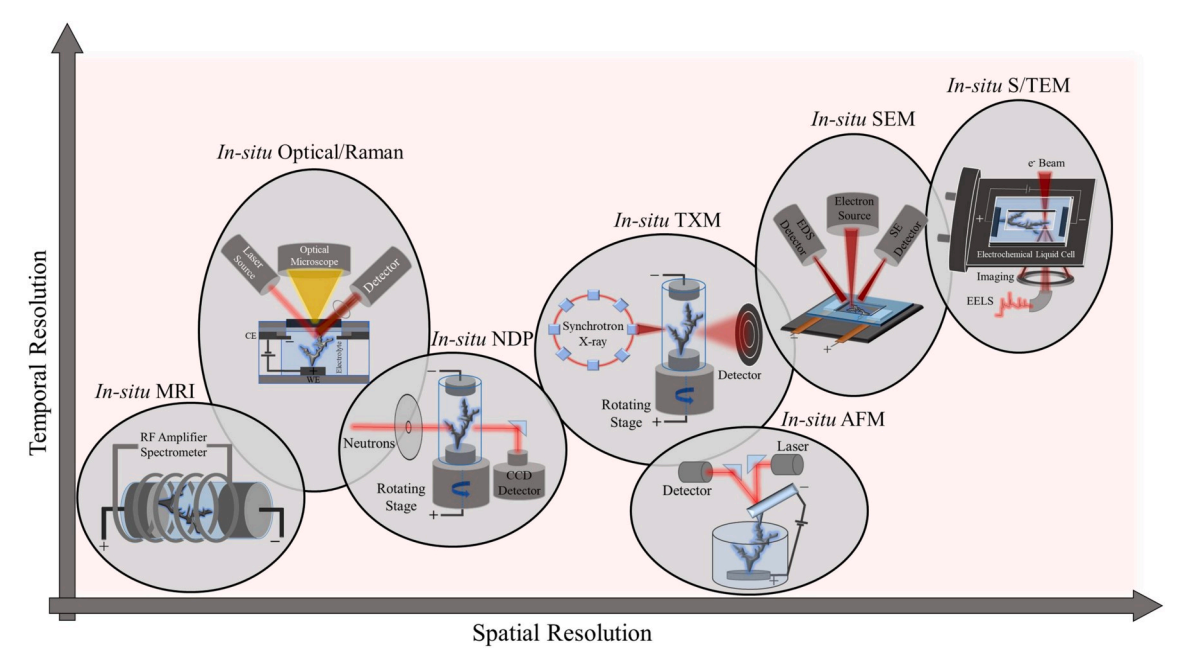


Fig. 3. In-situ/operando imaging techniques with respect to their comparative spatial and temporal resolutions. The techniques include MRI, optical/Raman, NDP, TXM, AFM, SEM and TEM and their in-situ cell designs used for studying Li dendrites are shown schematically.

orbital (LUMO) levels) and the Fermi level Li, electrons tend to transfer from Li to the unoccupied orbital of the electrolyte and reduce the electrolyte at the Li/electrolyte interface [29]. This thin SEI layer has the properties of an ideal solid electrolyte, beacuses it is electronically insulating but ionically conductive, with the thickness ranging from few to hundreds of nm determined by the electron tunneling range [30].

Different from the intercalation and alloying type electrode materials (such as carbon and silicon), Li is a hostless anode material with infinite relative volume change upon cycling. This means that the volumetric ratio of Li metal at charged state to the discharged state is infinite. As such, the naturally formed SEI layer that is not flexible enough and does not satisfy the Monroe and Newman's double shear modulus limit [20], cannot accommodate such large volume change and breaks under the induced stress favoring formation of randomly oriented Li dendrites (Fig. 2D) [31]. It is also speculated that the SEI layer has a heterogeneous and non-uniform composition, which results in local variation in mechanical stability and ionic conductivity. Therefore, random fractures in the SEI layer and unequal ionic flux excels the inhomogeneous and local deposition of Li dendrites [32]. Liu et al. [33] recently modeled the effect of evolving SEI thickness on the lithium electrodeposition reaction and suggested that flat lithium surface, uniform SEI layer, and low SEI ionic resistance are key factors in homogeneous Li deposition.

3. In-situ and operando imaging techniques

For decades, the understanding of the Li dendrite growth mechanism was highly reliant on the theoretical calculations. However, the models developed through numerical simulations may overlook some of the influential parameters, thus could deviate from the working conditions of electrochemical systems. There have been many experimental evidences demonstrating that the complexity of Li-dendrite formation mechanisms is beyond the developed models and there are ambiguities yet to be discovered before we can fully understand this phenomenon. Hence, the development of advanced materials characterization methods capable of imaging and monitoring various stages of Li dendrite formation and growth could greatly contribute to achieving a comprehensive understanding about major phenomena that were predicted to cause Li dendrite formation. Therefore, understanding, prediction and suppression of Li dendrite formation have been reexamined through the

newly discovered imaging techniques at various scales to help researchers in finding solutions to address the Li dendrite growth issue.

Although *ex-situ* characterization techniques could provide valuable information about the Li metal anode structure and composition, the highly reactive nature of Li and its moisture/air sensitivity brought many challenges and artifacts to *ex-situ* studies of Li dendrites. Therefore, in the recent years, experimental imaging and analysis of Li dendrites were sought mainly under *in-situ* and *operando* conditions to obtain realistic understandings of the Li dendrites growth behavior.

The Latin phrase in-situ (as opposed to ex-situ), means "on site", which indicates that the material is studied in its original/natural state or in a chemical environment that replicates its service environment. On the other hand, operando means "under operation", so ideally the operando experiments refer to studying the materials during their service condition, such as charging and discharging for the battery materials. In other words, imaging the Li deposition periodically by pausing the current/voltage and then restarting it, is considered as an in-situ experiment, while uninterrupted study of Li formation under operation is called an operando measurement. Utilization of non-invasive operando monitoring techniques can provide valuable information about the behavior of Li electrodes, which are free of potential artifacts caused by ambient and moisture exposure of Li metal after cell disassembly. Exploring the correlation between electrode materials structure, cell design and electrochemical performance under operando electrochemical conditions can allow for finding accurate cause-and-effect relationship and reaching clearer conclusions about the failure mechanisms of Li metal batteries. Besides differences, in-situ and operando are generally used interchangeably in literature. In-situ/operando imaging techniques can evaluate the existing theories about Li dendrite growth and contribute to the discovery of more developed and comprehensive models, based on which effective Li dendrites mitigation strategies can be invented. The development of reliable in-situ/operando methods is a non-trivial and complicated task that require special design of the electrochemical cells and probing equipment, so special considerations should be applied to prevent any significant artifacts affecting the interpretation.

In this work, we carried out a comprehensive review on recent studies involving Li dendrite formation and growth mechanisms revealed by microscopy and imaging techniques. These

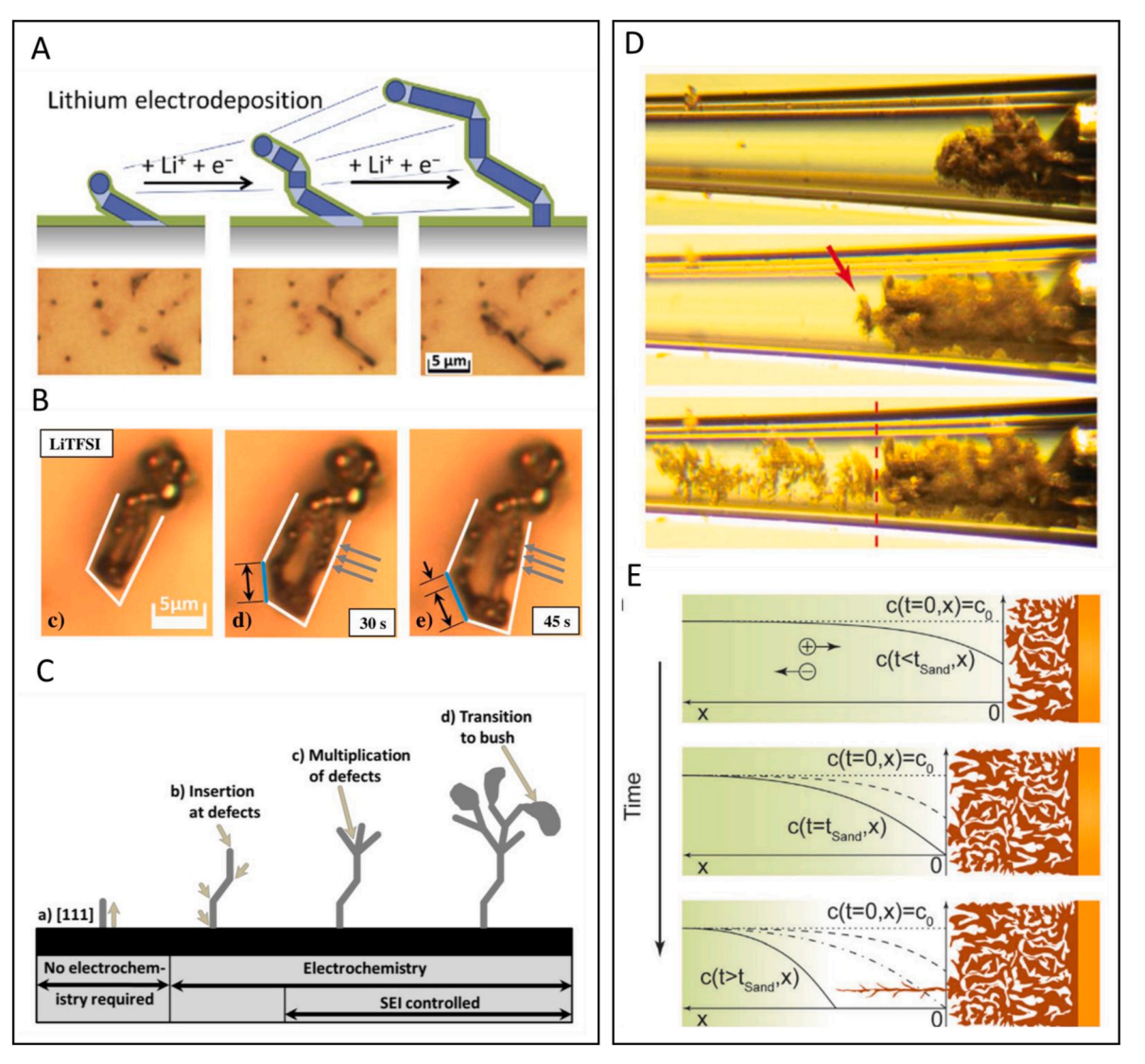


Fig. 4. Representative figures of *in-situ/operando* optical microscopy results on Li dendrite growth. (a) Insertion of Li atoms either from the base, at kinks or in a region at the tip of deposited Li in IM LiPF₆ in EC/DMC electrolyte: Reproduced with permission [47]. Copyright 2014, Elsevier; (b) Spherical deposition of Li in 1 M LiTFSI in DOL/DME electrolyte: Reproduced with permission [50]. Copyright 2015, Elsevier; (c) Transition from Li filament to bushes under the effect of crystal structure, electrochemistry and SEI: Reproduced from [51]. Transition from mossy to dendritic Li by (d) optical microscopy and (e) theoretical calculations: Reproduced with permission [45]. Copyright 2016, The Royal Society of Chemistry.

characterizations include optical, electron, X-ray, scanning probe, neutron and resonance-based microscopies. Fig. 3 shows configuration and design of different in-situ/operando imaging techniques used for studying the deposition of Li dendrites, with respect to their spatial and temporal resolutions being limited by the physics of the probing or exciting beam. The temporal resolution provides information over time spans that the reactions can be observed, which is generally limited by the signal-to-noise ratio of the technique. While spatial resolution is the sampling interval of the microscopy techniques in the spatial domain. Optical and nuclear-magnetic based imaging techniques have lowest spatial resolution, while electron microscopy has the highest. While, the spatial resolution of X-ray, atomic probe and neutron-based imaging techniques lie in between. This review focuses on the in-situ/operando imaging techniques used to study Li dendrites. The operating principles and details of in-situ cell designs, are described elsewhere [34,35]. The Li growth mechanism understandings from each imaging technique is elaborated here, and possible future research directions are provided. Recent developments on spectroscopy and imaging of other battery materials can be found elsewhere [35-37].

3.1. In-situ/Operando optical-based imaging techniques

3.1.1. Optical microscopy

In-situ optical imaging and analysis have been utilized intensively to study the Li-electrodeposition behavior and dendrite growth. This is because in-situ optical imaging is the most accessible in-situ imaging method and can be simply made on a glass vial. In-situ holographic interferometry, which is able to detect changes in the concentration of chemical species, is a strong method in the study of Li dendrites. It is known that the sudden and uncompensated decrease in the Li⁺ concentration at the Li/electrolyte interphase reflects the formation of Li dendrites [38-40]. Therefore, by using holographic interferometry, valuable insights about the mechanisms and steps of Li-dendrite growth such as the incubation time and the diffusion layer development, correlated with Li⁺ concentration changes, has been obtained. In addition, the effect of parameters such as applied current density, water contamination content and the choice of electrolyte on the dendritic deposition of Li could be monitored. Through such studies it was demonstrated that the dendrite growth incubation time decreases significantly by increasing the current density and the recorded

incubation times are in good agreement with calculated values based on Sand's theory. Nonetheless, utilizing microscopy techniques, it is shown that Li dendrites can start to grow before the surface Li⁺ concentration drops to zero [41,42]. This indicates that the surface concentration is not the only parameter responsible for the Li dendrites evolution. Nishikawa et al. [43] suggested that initial surface state and chemistry of the substrate together with Li⁺ depletion are the responsible factors in both organic and ionic liquid electrolytes. They demonstrated that the length of the dendrites is controlled by ionic mass transfer and follows a linear growth rate with square root of time and the slope changes drastically after depletion of Li⁺ ions. Even though it can provide valuable information regarding morphological changes of Li during plating/stripping close to commercial battery environment, there are some drawbacks associated with in-situ optical imaging of Li dendrites. Important challenges are the detrimental effect of electrically non-conducting and opaque electrolyte on the image quality, especially at high magnifications, and the poor resolution of optical microscopy. This is fundamentally restricted by the diffraction limit of the visible light, which makes it challenging to monitor microstructural changes. Therefore, laser scanning confocal microscopy (LSCM) with superior optical resolution and contrast was utilized for the in-situ optical microscopy study of Li dendrites growth. Using this technique, the effect of electrolyte [42] and electrolyte salt compositions [44] on the morphology and structure of Li dendrites were studied. It was realized that Li morphology is also dependent on the SEI layer composition together with ionic mass transfer rate [42,44]. It was shown that at low current densities ($<2 \mu A$ cm⁻²) the deposition morphology of Li does not follow the branch-type morphology of Li dendrites predicted, but a mossy/bush structure is observed [45]. Yamaki et al. [46] for the first time identified the root based growth of Li whiskers, which was not expected from the typical growth models of dendrites. They attributed this behavior to internal stress that can be released on the lithium electrode beneath the SEI layer. Later, Steiger et al. [47,48] studied the deposition behavior of mossy Li further and proposed that the deposition not only happen at the base, but Li atoms can insert into the crystal at the crystalline defect sites, as well (Fig. 4A). This behavior disputes the conventional explanations of Li dendrite growth based on field and concentration gradients. Here they suggested the major role of SEI. The thick SEI shell formed at the tip of the whiskers holds the structure at the same position on the tip and Li can insert from the more freshly formed thin SEI at the grain boundaries (kinks of needles) or in between lithium particles and stress-mediated diffusional transport promotes whisker growth. Different morphologies of Li has been observed in different electrolytes, which imply the role of SEI composition and morphology on the deposition behavior of Li [44,49,50]. They observed a more spherical Li deposition in case of LP30 1 M LiTFSI (lithium bis(trifluoromethanesulfonyl)imide) in DOL/DME (1,3-dioxolane/1,2- dimethoxyethane) compared to 1 M lithiumhexafluorophosphate LiPF₆ in EC/DMC 1:1 and concluded that different SEI composition formed in LiTFSI-containing electrolyte leads to the more spherical Li deposition (Fig. 4B) compared to the filament shaped Li formed in LP30 (Fig. 4A). Steiger et al. showed that Li filaments could grew even in the absence of electrolyte and under insertion mechanism during thermal evaporation deposition [50]. This behavior suggests the independency of Li filaments growth to SEI and electrolyte and adds the role of lithium diffusion and crystallization as key processes to be considered for controlling the deposition behavior of Li. Steiger et al. [51] suggest that the early stages of Li deposition is in the form of filaments; then growth continues by a lithium insertion mechanism at the Li crystalline defect sites; once the defects sites increases and the effect of SEI becomes more significant, branching and transition from filament to bush occurs (Fig. 4C). Besides, Bai et al. [45] reveled transition from mossy to dendritic deposition utilizing a novel capillary cell (Fig. 4D). The striking differences in morphology and dynamics imply that Li growth can follow two different mechanisms of reaction limited and diffusion limited. Relatively dense mossy Li grows in a reaction-limited manner and follows with a diffusion-limited dendritic Li deposition.

during concentration polarization. Based on Sand's time formula, the dendrite initiation time τ is in an inverse relation with J [2]. It has been known that by applying higher current densities, dendritic deposition of Li initiates at an earlier stage. However, Bai et al. [45] incorporated the effect of deposition time in the morphologic transition of Li, as well. Based on their *in-situ* observations Sand's capacity term ($C_{Sand} = JT_{Sand}$) was developed. They correlated the beneficial effect of high concentration (larger c_0) and lithium ion diffusivity (D) of electrolyte, large active surface area (A) and low current density (I) to higher Sand's capacity and engineering rechargeable high-rate and large-capacity lithium metal anode ($C_{Sand} \sim \frac{ADc02}{I}$). Monroe and Newman proposed that the Li growth rate at high current density increases exponentially and high current density worsens the dendritic deposition of Li [19], which was confirmed by in-situ optical and electron microscopy characterizations. Many researches have shown the effect of current density on the deposition behavior of Li, showing faster transition of mossy to dendrites [52,53]. However, based on in-situ optical imaging results the high current density is not detrimental at all the stages of Li deposition. The higher current density leads to higher number of electrodeposition sites beneficial at the nucleation stage [44,54,55]. The nature of Li deposition has been recently shown to be also dependent on the proximity of the current collector to defects. Porz et al. [56] have shown that above a critical current density, Li can penetrate/infiltrate at the defect sites and move in solid electrolyte leading to short circuit. This behavior has been shown to be consistent for amorphous (70/30 mol% Li₂S–P₂S₅), polycrystalline (β-Li₃PS₄) and crystalline (Li₆La₃ZrTaO₁₂) solid electrolytes and independent of the shear modulus of electrolyte. They proposed an electrochemomechanical model for plating and penetration of Li in the presence of solid electrolytes. This is inconsistent with the theoretical calculation of Monroe and Newman [57] where they predicted that Li dendrites can be completely suppressed by having an interface with shear modulus of at least twice of Li (shear modulus of Li

Fig. 4E shows the theoretical explanation of the Li growth mechanisms

Spatial variations in reaction kinetics can result in the morphological evolution of the Li metal electrode. Utilizing in-situ optical microscopy Li dendrite progress is directly related to the shape of voltage traces and has been used to interpret the electrical signals [9,59]. Voltage peaks observed during dissolution stage is correlated with the formation of pits in the bulk Li electrode. Utilizing continuum-scale modeling together with operando optical microscopy, Wood et al. [9] provided explanation about dendrite nucleation and evolution as a function of time, surface pitting during Li electrodissolution and kinetic parameters that affects the overpotential over the course of Li morphological alteration. During dissolution process formation of electrochemically insulating Li "dead Li" was also observed with in-situ optical microscopy [48,60]. By concurrently characterizing the Li growth evolution and electrical characteristics, different types of short circuits showing differently in electrical signal, were detected [59]. Complete short circuit happens when the two electrodes are fully connected by Li dendrites and the voltage drops to zero, while soft short-circuit happens when Li dendrites are regarded as contact fuses and a drop in voltage without reaching to zero is detected. In this condition the current passes through the small physically connected areas and rises temperature, which leads to the local melting of the short-circuited dendrite and connection breakage.

3.1.2. Raman imaging

is 4.2 GPa) [58].

Raman spectroscopy is composed of a conformal microscope combined with a spectrometer that can be used to obtain spectra from a specific spot on sample. Raman spectroscopy allows for identifying the vibrational energy of molecular/crystal bonding, which are defined by crystal symmetry, structural (dis)order and strain [61]. Since Raman spectroscopy can detect Li⁺ by Li⁺-solvent interactions [62] or anion concentration by "electro-neutrality" concept [63], it is considered a great technique to study the correlation of Li dendrite growth with Li-ion

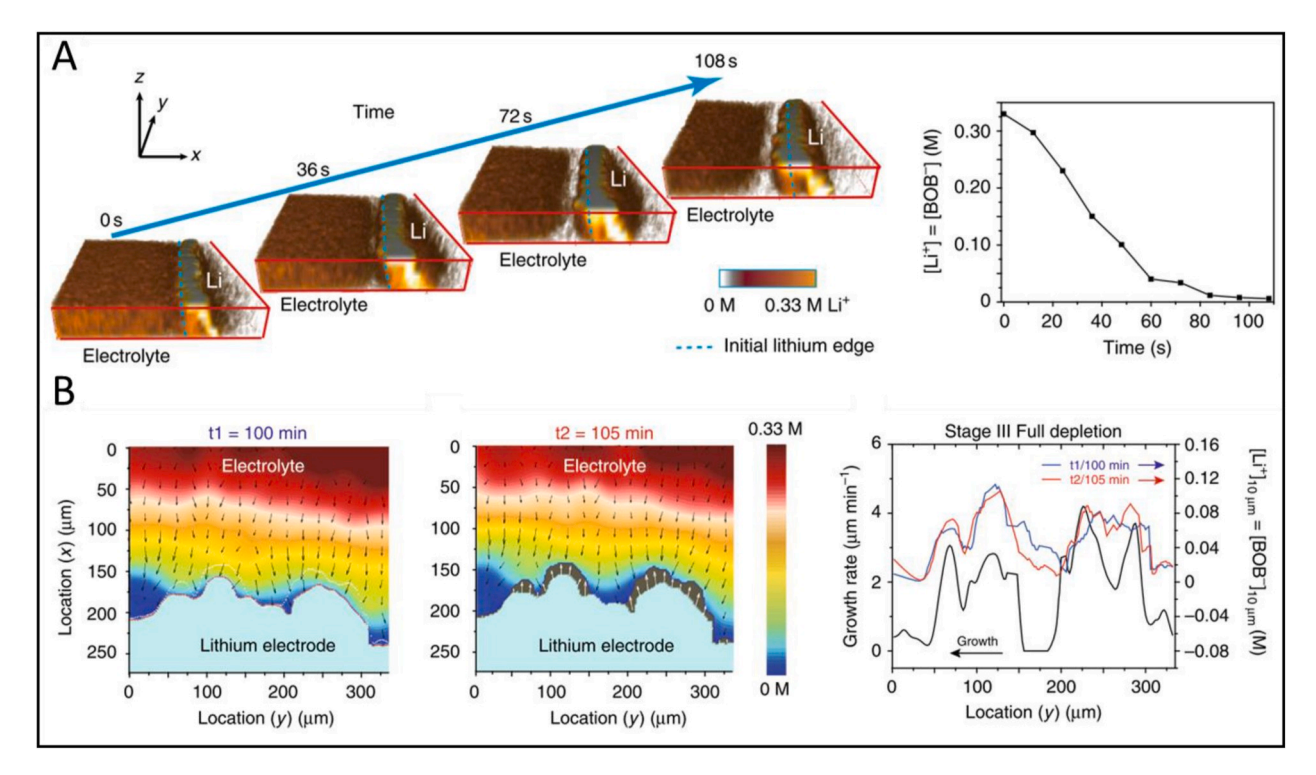


Fig. 5. Representative figures of in-situ Raman imaging results on Li dendrite growth. (a) 3D visualization of ion transport/depletion and dendrite growth on Li metal electrode (left). Average Li⁺ concentration 5 µm away from the Li surface (right): Reproduced with permission [65]. Copyright 2018, Springer Nature; (b) Correlation between Li growth and Li⁺ concentration at two representative moments: Reproduced with permission [65]. Copyright 2018, Springer Nature.

concentration gradient in the electrode/electrolyte interphase. As mentioned earlier uneven Li-ion concentration and its depletion at the electrode/electrolyte interphase were considered as correlating phenomena with the formation of Li dendrites. Although, Raman spectroscopy and imaging have many advantages over conventional optical microscopy methods, including high contrast/spatial resolution, valuable bonding/chemical information and ability to analyze materials with poor crystallinity, it suffers from low spatial and temporal (~ 10 min per frame) resolution.

Confocal Raman microspectroscopy (CRM) utilizes a confocal aperture, which can achieve $<1~\mu m$ lateral and $\sim 8~\mu m$ axial spatial resolution, and is capable of collecting optical sections from thick samples [61]. Accordingly, the correlation between the Li⁺ concentration gradient and Li dendrite formation was confirmed by CRM in Li/polymer electrolyte symmetric cells [63]. In addition, the diffusion coefficient of Li ion in liquid electrolytes such as DMC in various concentration regimes could be measured using CRM. However, Raman confocal microspectroscopy cannot be applied for accurate 2D cartography of concentration. In the same system, in-situ optical absorption of an anion in the electrolyte were used based on the assumption that a linear relationship exists between the absorption and the ionic concentration [63]. Also, in-situ gradient-sensitive optical detection was used to characterize variations in optical index near the electrode surface correlated to concentration gradients [63]. It should be noted that in-situ measurement of lithium ion concentrations with Raman spectroscopy is challenging since Li⁺ does not contain accessible optical signatures like fluorescence or active vibrational modes [62].

Poor temporal resolution of spontaneous Raman, which is limited by signal/noise ratio of the system, cannot follow rapid changes in electrolyte concentrations. Therefore, the stimulated Raman scattering (SRS) microscopy, which utilizes spatially and temporally synchronized picosecond laser pulse trains and achieves 10^8 times higher temporal resolution (compared to the conventional Raman spectroscopy) and high spatial resolution of ~ 500 nm was utilized for *in-situ* mapping of Li concentration profile and study of Li-dendrite growth [64]. This

technique utilizes two synchronized beams: a pump laser beam with a constant frequency and a Stokes laser beam with a scanning frequency. When the difference between the two beams is equal to the vibration transition of the exposed material, the occurrence and probability of such transition is significantly increased and can be detected in a considerably smaller acquisition time. By introduction of SRS microscopy with high sensitivity (<0.5 mM), fast imaging rate (~2 μ s/pixel) and acceptable spatial resolution (300-500 nm) additional insights about the Li dendrite growth mechanism were achieved. As such, Cheng et al. [65] demonstrated that the Li dendrite growth follows a three-stage process namely mossy Li deposition, mixture of mossy Li and Li dendrites, and eventually Li dendrite formation that occur sequentially as a function of Li concentration at the interphase. Using this technique, the effectiveness of artificial SEI layers and electrolyte additive on suppressing or delaying the dendrite growth at each specific stage has been also evaluated. Fig. 5 is a visualization of ion transport/concentration and its correlation with dendrite growth. SRS images in Fig. 5A clearly has resolved the Li ion depletion regime near the Li electrode surface that allows simultaneous observation of Li ion depletion and uneven deposition of Li. The right panel in Fig. 5A shows the average Li ion concentration 5 µm away from the Li metal anode surface. Fig. 5B show the temporal evolution of Li microstructure (with interval of five minutes). The left panel shows the solid Li electrode at t1=100and t2 = 105 min in turquoise with the corresponding Li^+ distribution above it. The arrows in the electrolyte denotes the local concentration gradient. Fig. 5B right panel shows Li at t1 in turquoise, the Li⁺ distribution at t2 and its growth between t1 to t2 in dark gray.

3.2. In-situ/Operando electron-based imaging techniques

3.2.1. Scanning electron microscopy

Scanning electron microscopy (SEM), utilizes a raster scanning of focused electron beam that probes the surface of sample and provides topographical compositional information through detection of secondary and backscattered electrons and generated X-rays. *In-situ* SEM is a

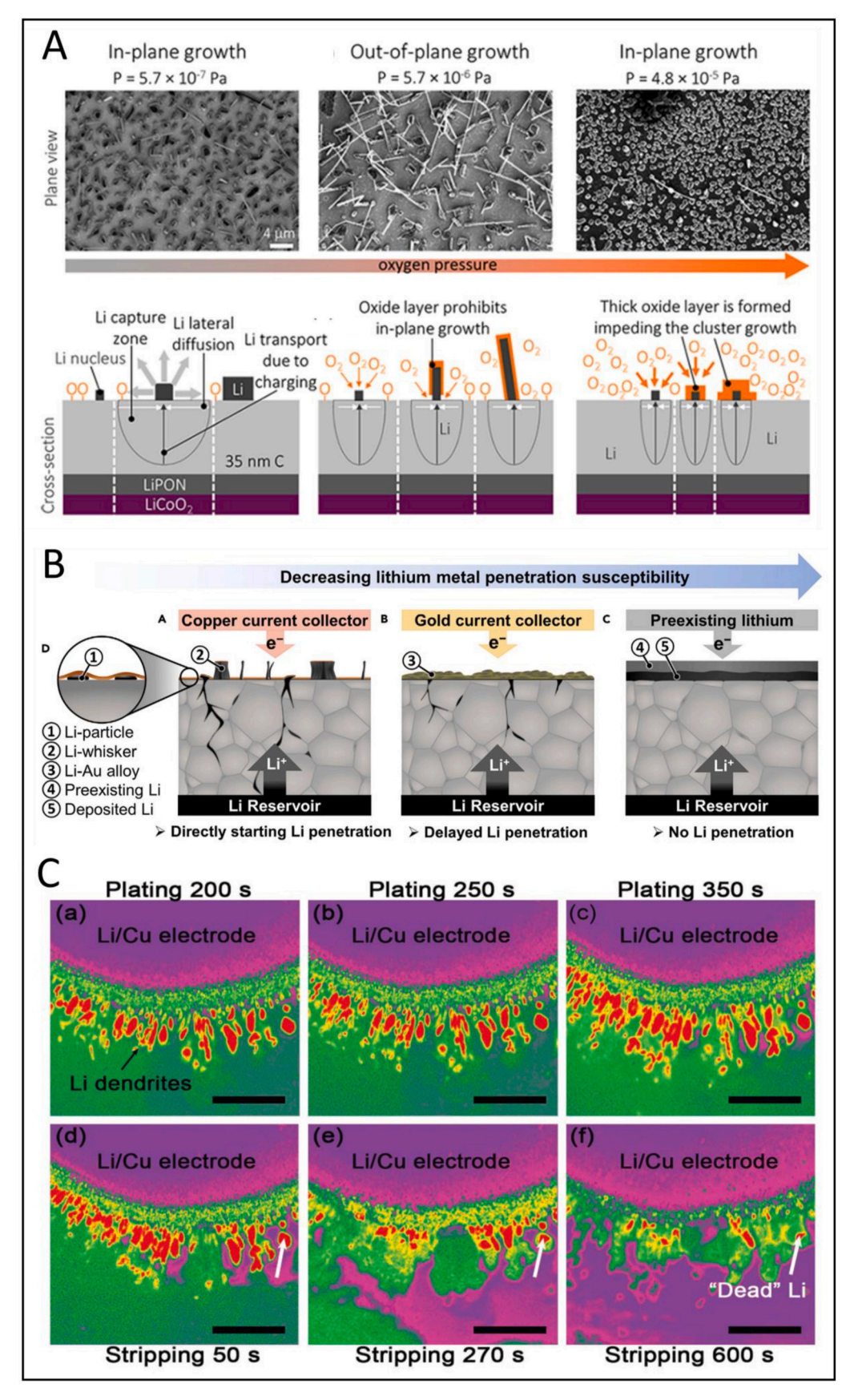


Fig. 6. Representative figures of in-situ/ operando SEM results on Li dendrite growth. a) Effect of the residual oxygen pressure on in-plane and out-of-plane Li deposition behavior: Reproduced with permission [72]. Copyright 2018, American Chemical Society; (b) Li plating behavior using different current collector materials in contact with LLZO solid electrolyte: Reproduced with permission [77]. Copyright 2019, Elsevier; (c) Time lapse series of SEM images of the lithium plating and stripping processes in the presence of LiNO₃ additive: Reproduced with permission [78]. Copyright 2017, John Wiley and

reliable technique for studying the Li dendrites due to very higher spatial resolution compared to optical systems, and, on the other hand, much lower beam damage and simpler cell design compared to transmission electron microscopy. However, the penetration depth of low kV electron beam is very limited, and the information is limited to the outer surface of the samples, making imaging restricted to open/electron-beam transparent cells. *In-situ* SEM study of Li dendrites evolution and growth requires specific cell design and operation under high vacuum environment, which limits the electrolyte choice to less volatile ionic liquids and polymeric/solid electrolytes.

Orsini et al. [66] used a semi in-situ SEM technique utilizing air-tight transfer chamber and also a cooling stage to study the Li dendrite morphology in high resolution and under different current densities. Following that work, in-situ SEM was widely used to study the Li deposition behavior in the presence of ionic liquid and solid electrolyte [67-69]. The plating of Li at the interface of Li/solid electrolyte was studied to evaluate the mechanisms of Li dendrite nucleation, growth and stripping in solid state batteries (SSBs) under different current densities [68,70-73]. It was shown that the Li nucleation rate increase with increasing the current density [70]. At low current densities the Li nucleation happens sparsely at the Li/solid electrolyte interface, which later on develops into Li fibers [74]. Meanwhile, the low current density $(50 \,\mu\text{A cm}^{-2})$ during the Li stripping leads to uniform deflatation of the Li fibers form head to bottom and only a thin surface skin remained un-stripped, which was further verified to be the SEI layer [75]. Utilizing in-situ SEM imaging, it is shown that the localized cell pressure and also oxygen partial pressures can significantly affect the Li deposition behavior at the solid electrolyte interface as well [71,72]. The results convey that the homogeneous pressurization of the sample at the Li/solid electrolyte interface is a critical factor for a stable charge/discharge process [71] and the presence of residual oxygen can significantly affect the Li deposition morphology [72]. Filament-type (1D) growth of Li will be promoted at an intermediate O2 level (partial pressure of $\approx 10^{-6}$ Pa) due to formation of a thin oxide sheath around the growing Li (Fig. 6A). The bewildering mechanism of Li penetration through solid electrolytes, which has been evaluated by in-situ optical and also neutron imaging [56,76], was also evaluated by in-situ SEM analysis [77]. A comprehensive prediction by including the possible micro non-uniformities in the interfacial kinetics that depends on surface microstructure was proposed by Krauskopf et al. [77] Utilizing ex-situ and in-situ SEM imaging. Fig. 6B shows how the behavior of Li electrodeposition can change by altering the current collector properties. It is shown that defect sites introduced by mechanical damage can severely affect the deposition behavior. Also utilizing alloy forming metals (like gold) can reduce nucleation barrier for deposition of Li and form more uniform Li and delay penetration of Li through solid electrolytes. However, the Li penetration through the current collector was still observed. On the other hand, utilizing a small Li metal reservoir can diminish the driving force for heterogeneous nucleation and prevents the penetration of Li through solid electrolyte and short-circuiting the battery. Noteworthy such results have challenged the theoretical assessment of Newman and Monroe on Li dendrite suppression with solid electrolytes in case of inorganic solid electrolytess [77].

Tang et al. [69] used a special assembly using a thin layer of carbon as a local current collector that is able to physically isolate the ionic liquid, meanwhile allows Li to diffuse through. In this assembly concentration polarization effect will be lessened. This will allow for a better clarification of the effect of stress and mechanical force imposed by oxide layer and SEI, thus can drive Li morphological evolution from root through diffusional stress relaxation. The first in-situ SEM characterization of the Li dendrite growth in volatile electrolytes was performed in 2017 by Rong et al. [78] Using the EC-SEM liquid cell, they studied the effect of different additives (lithium nitrate (LiNO3) and lithium poly-sulfide (Li₂S₈)) on the lithium dendrite growth. The false-colored map in Fig. 6C shows the growth of dendrites and its partial dissolution under a reversed current. The unchanged Li particles that

were observed after fully discharging the cell confirm the formation of dead Li. It was also demonstrated that LiNO $_3$ can form a desirable SEI and Li $_2$ S $_8$ etches away "dead" Li. Based on the comparison between length and density of dendrites in the presence of additives, they proposed the effective suppression of Li dendrites by using Li $_2$ S $_8$ and LiNO $_3$ as co-additives in the LiTFSI/DOL/DME electrolyte. Recently, Meng et al. [79] identified the formation mechanism of dead Li in different types of electrolytes and quantified the contributing amount of unreacted metallic Li (Li 0) to the whole dead Li amount. Utilizing cryo-FIB-SEM and cryo-TEM results, they showed that dead Li consist of both electrochemically formed Li $^+$ compounds in the SEI and isolated metallic Li 0 . They proposed that dendritic Li microstructures with high morphological tortuosity are more prone to trap unreacted metallic Li 0 in SEI during the stripping process.

Utilizing an *in-situ* nanomechanical device integrated in an SEM system, Xu et al. [25] calculated the Yield strength of polycrystalline bulk Li and also Li whiskers. Their analysis shows the Yield strength of bulk Li to be about 1 MPa, but about 100 MPa is case of narrow Li dendrites. Also, it is mentioned that mechanical stability is highly dependent on crystallographic orientation of Li dendrites. This can be one reason why "double shear modulus theory" of Monroe and Newman is not applicable in commercial batteries and explains how the Li dendrites penetrate through some solid electrolytes with much higher shear modulus that what was calculated for bulk Li.

3.2.2. (Scanning) Transmission electron microscopy

Different from SEM, transmission electron microscopy (TEM) relies on an electron beam with much higher voltage that can transmit through a thin sample and form images with ultrahigh spatial resolution. Besides detailed morphological information, TEM provides phase contrast images revealing the crystalline structure and chemical composition of materials at the atomic scale. The development of in-situ TEM is a major breakthrough in the field of in-situ techniques for battery research and was initially designed by using an open-cell configuration [80]. Since volatile electrolytes are not compatible with the ultra-high vacuum of TEM columns, two types of open-cell configurations using either ionic liquids, with extremely low vapor pressures, or metal oxides (like Li₂O or LiAlSiOx) as the solid-state electrolyte are used for in-situ TEM experiments [80,81]. However, the utilization of open cells to study the Li dendrites have disadvantages such as large deviation from commercial cell conditions, which can lead to invalid conclusions. Interfacial stability of Li with solid electrolyte was studied through S/TEM imaging, identifying the formation of an interlayer between Li and electrolyte that can add interfacial resistance over cycling. This is a result of localized cathodic behavior of the solid electrolytes like LLZO that become in contact with Li [82,83]. In 2011, our group used in-situ transmission electron microscopy (TEM) technique for the first time to observe the Li dendrite growth in nanoscale Li-ion batteries [81]. Through the clear observation of Li nucleation and growth at the anode/electrolyte interface, it is shown that Li fibers grow at the tip of nanowire with locally enhanced electric field and grows parallel to the direction of the applied electric field [80,81].

In the initial studies an ionic liquid -based electrolyte with low vapor pressure was used instead of the practical liquid electrolyte and the study was performed on nano-batteries, which can be different from real battery conditions. Therefore, development of vacuum-tight, electron-transparent environmental cells for TEM has always been a key in improving the *operando* investigations of Li dendrite growth mechanism. Liquid cell studies with scanning/transmission electron microscopy (S/TEM) approach employs electrodes that are microfabricated onto a silicon electrochemical microchip device such that the desired electrodes can be interfaced with a potentiostat by means of electrical contacts in a TEM holder [84]. *In-situ* electrochemical liquid cell transmission electron microscopy (TEM) allows imaging chemical reactions in liquids with high spatial resolution that can be used to study the thin SEI layer on the electrodeposited Li [84–86]. The previously studied nucleation

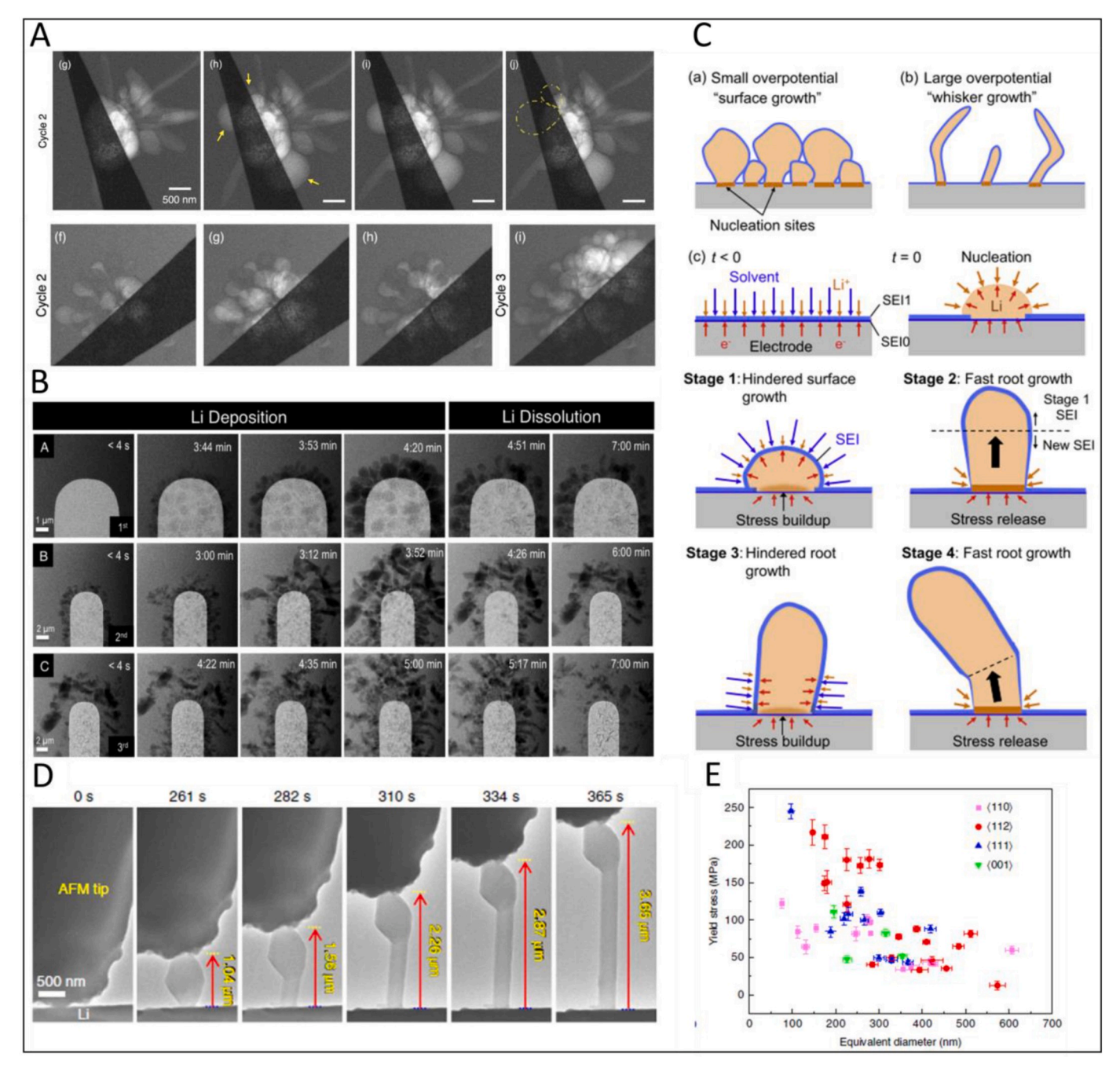


Fig. 7. Representative figures of *in-situ/operando* S/TEM results on Li dendrite growth. (a) Time series of Li electrodeposition and stripping images taken every minute (top row) showing needle like morphology and every 15 s (bottom row) showing spherical geometry: Reproduced with permission [91]. Copyright 2015, American Chemical Society; (b) High-angle annular dark field (HAADF) images of Li deposition and dissolution over three subsequent charge/discharge cycles of the operando cell: Reproduced with permission [89]. Copyright 2015, American Chemical Society; (c) Schematic illustration explaining root growth mechanism of lithium whiskers observed by in-situ SEM imaging: Reproduced with permission [86]. Copyright 2017, Elsevier; (d) In-situ AFM-ETEM imaging of Li whiskers root growth: Reproduced with permission [26]. Copyright 2020, Springer Nature; (e) Yield strength of Li whiskers with different diameters and growth directions: Reproduced with permission [26]. Copyright 2020, Springer Nature.

and growth of copper (Cu) and lead (Sn) dendrites using *in-situ* electron microscopy in liquid cells were the motifs for studying Li electrodeposition in commercially used electrolytes [87,88]. However, use of electrolytes with high vapor pressures (like LiPF $_6$ in organic solvents) is difficult and additionally due to low atomic number, Li has low contrast when imaged through the membrane windows. Zeng et al. [84] utilized electrochemical liquid TEM cell and visualized Li dendrite and SEI formation. An important aspect of Li metal degradation is the formation of SEI passivation film due to the reduction of the electrolyte solvent at the Li/electrolyte interface. Of particular importance for STEM imaging is

the identification of an image contrast reversal that can differentiate between solid Li, SEI and the surrounding liquid electrolyte [89]. In bright-field STEM imaging (background with zero scattering show bright), materials with higher atomic number or thickness appear darker and the electrodeposited Li being less dense than the surrounding electrolyte show up darker and facilitates imaging. Utilizing chemically sensitive annular dark field STEM imaging it was discovered that the SEI is twice as dense as the electrolyte [85]. Based on *in-situ* electrochemical TEM studies, Sacci et al. [85] speculated that the non-uniform ordering of the SEI in LiPF₆/EC/DMC liquid electrolyte plays a role in the

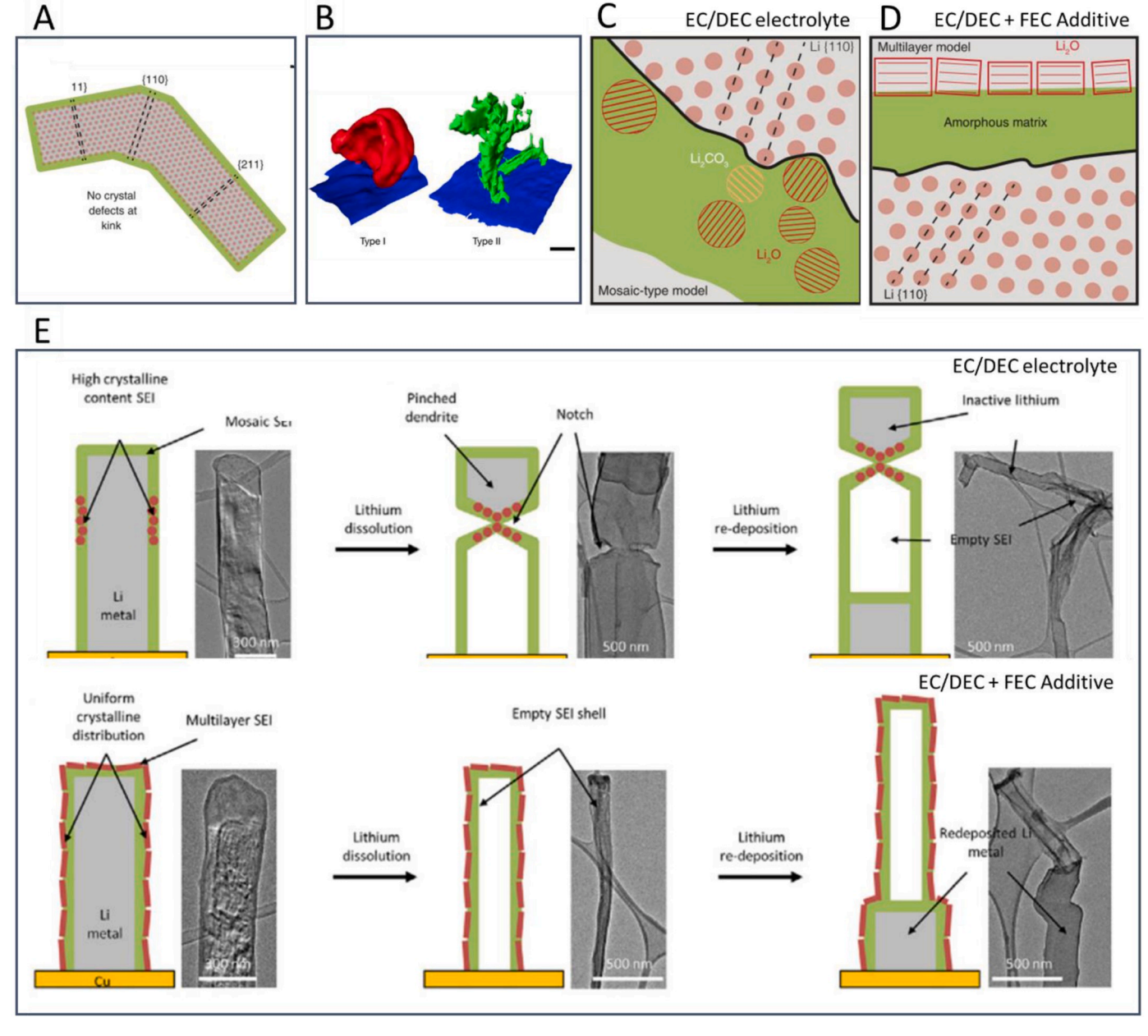


Fig. 8. Representative figures of cryo-TEM imaging results on Li dendrite growth. (a) Schematic of a lithium filament showing its single-crystalline nature changing direction at the kinks: Reproduced with permission [93]. Copyright 217, The American Association for the Advancement of Science; (b) Three-dimensional reconstructions of different structures of Li dendrites observed by cryo-STEM images obtained from cryo-FIB prepared samples: Reproduced with permission [94]. Copyright 2018, Springer Nature. Schematic of the observed structure formed on Li dendrites in EC-DEC electrolyte; (c) without and (d) with FEC additive with mosaic-type and multilayer models, respectively: Reproduced with permission [93]. Copyright 217, The American Association for the Advancement of Science; (e) Non-uniform Li Stripping through Mosaic SEI formed in EC/DEC electrolyte (top row) and uniform Li Stripping through multilayer SEI formed in EC/DEC electrolyte with FEC additive (bottom row): Reproduced with permission [106]. Copyright 2018, Elsevier.

subsequent Li dendrite morphology. These results which were also confirmed by Zhu et al. [90], demonstrated that the SEI formation was not uniform and had a random shape resembling that of Li dendrites. Zeng et al. [84] showed an initial fast growth of SEI film up to 200 nm, followed by stopped growth process, which suggests the low transport rate of electrons through the SEI film. Utilizing STEM dark field imaging the structural evolution of Li was studied under different current densities considering the effect of electron beam as well [91]. It was discovered that electron beam can accelerate surface film formation and generate a unique SEI that facilitates multisite nucleation of Li (Fig. 7A). The top row panels in Fig. 7A show needle-like Li growth behavior under *in-situ* imaging (one-minute intervals), which is different from the rounded nodules observed during *operando* imaging (every few seconds)

shown in the bottom row panels of Fig. 7A. Thus, considering the significant effect of electron beam on the deposition behavior of Li, it is important to carefully regulate the imaging conditions to obtain the most reliable data reagarding both surface SEI and also bulk Li dendrite. Mehdi et al. [89] used electron beam dose rate of \leq 0.3 electrons Å $^{-2}$ s $^{-1}$ for collecting high-angle annular dark field (HAADF) images shown in Fig. 7B that clearly show the Li deposition, stripping and formation of dead Li. Kushima et al. [86] presented *in-situ* environmental transmission electron microscopy (ETEM) observations of metallic Li protrusions growing from their roots or tips depending on the overpotential, which showed the voltage-dependent competition between lithium electrodeposition and SEI formation reactions (Fig. 7C). The conclusion from their research is that the rate of SEI formation can affect Li

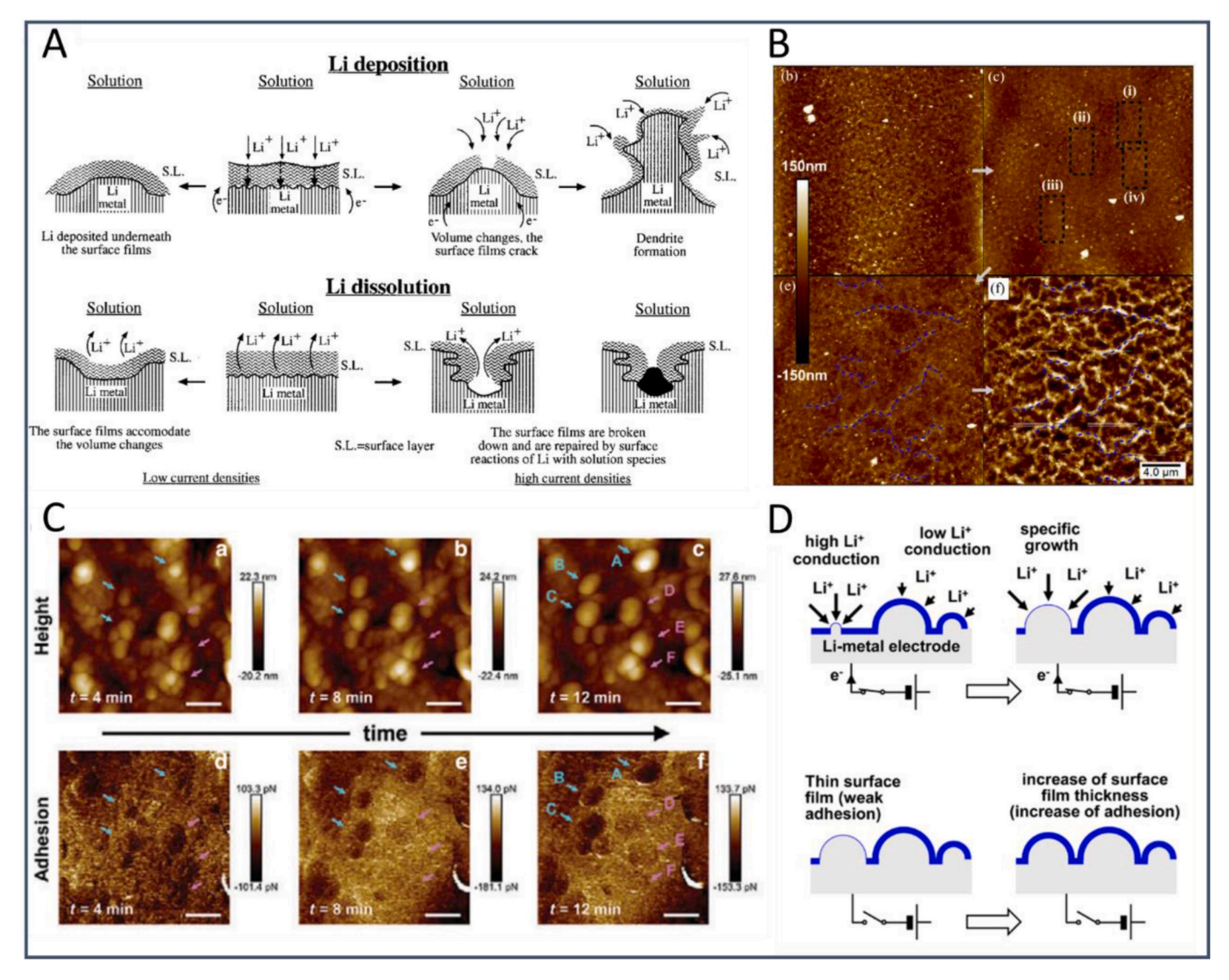


Fig. 9. Representative figures of *in-situ/operando* AFM results on Li dendrite growth. (a) An illustration of the effect of SEI on the morphological phenomena developed on Li electrodes during Li deposition and dissolution: Reproduced with permission [109]. Copyright 2000, American Chemical Society; (b) AFM images showing fracture/failure evolution in SEI at different strain levels: Reproduced with permission [111]. Copyright 2020, Elsevier; (c) Topographical (top row) and adhesion (bottom row) AFM images of the surface of the Li electrode at various times during the Li depositions process showing the local evolution of Li bumps: Reproduced with permission [108]. Copyright 2017, American Chemical Society; (d) A model for the mechanism of protrusion growth during Li deposition process (top row) showing preferred insertion of Li at high Li⁺ conducting points and in open circuit conditions (bottom row) showing thickening of the SEI layer: Reproduced with permission [108]. Copyright 2017, American Chemical Society.

deposition behavior. At low overpotentials, the rate of SEI formation is slower than the lithium deposition rate, and Li metal grows from the surface. At high overpotential and formation of thick SEI layer, when compressive stress at the root of Li deposits reaches a threshold, the SEI cannot sustain the applied stress, thus the intermittent volcanic eruptions activates the root growth mode. Slight separation of Li deposits from the original SEI, allows for easy diffusion of fresh lithium under the root, causing the whisker to extend and form kinked segments of nearly constant diameters. Also, they observed that root-grown dendrites are less stable during stripping due to the thinner SEI layer at the root and preferential stripping of Li from that area leading to easy formation of dead Li. The root growth mechanism under elastic constraint was very recently evaluated by He et al. [92] and Zhang et al. 26. By coupling an atomic force microscopy cantilever into a solid open-cell set-up in environmental transmission electron microscopy (AFM-ETEM), they studied the nucleation and growth mechanisms of Li whiskers under mechanical constraints that resembles the effect of separator/solid electrolyte pressure on Li dendrite growth. The geometrically

unchanged tip of the whiskers (Fig. 7D) during the growth process indicates the root-growth mode. He et al. [92] showed that Li whiskers can yield, buckle, kink or stop growing under specific elastic constraints. Also, Zhang et al. [26] evaluated the yield strength of Li whiskers to reach as high as 244 MPa (Fig. 7E), which is much higher than the previously measured strength of 105 MPa using *in-situ* SEM [25].

3.2.3. Cryo transmission electron microscopy

As mentioned earlier, Li metal samples are highly sensitive to electron beam damage, thus obtaining intrinsic information about Li dendrite growth mechanism without introducing any artifacts is a challenging task. Extensive high-energy beam of TEM can either destroys Li samples or induce artifacts leading to doubtful conclusions. High energy electron beam can break the sample bonds (primary damage) and produce secondary electrons and free radicals (secondary damage). Reducing the radiation damage has always been important in studying beam sensitive materials like Li that can be achieved by either reducing the exposure of sample to electron beam or by cooling the

sample. Dose reduction can be achieved by capturing images at high frame rates, by utilizing direct electron detection cameras, which can significantly reduce the beam dose and improve the signal to noise ratio. On the other hand, cryogenic electron microscopy (EM) allows for imaging of the structure of the light compounds like Li and its SEI at the nano scale. Inspired by structural biology characterization by cryo-TEM, Cui et al. [93] and Meng et al. [94], developed protocols for studying highly sensitive Li microstructures at liquid nitrogen temperatures (-170C). The strategies for preserving the pristine structure of Li metal anode during sample preparation, transformation, and imaging are discussed elsewhere [95]. It is shown that while standard TEM conditions result in sample degradation even at low dosage, cryo-EM enables high resolution imaging of Li samples even at high beam exposure times. They discovered that Li initially nucleates as amorphous phase [94] and later on develops into single crystal with specific growth directions (Fig. 8A) [93]. Kourkoutis's group identified two different types of Li dendrites [96,97]. They concluded that Type I dendrites are thicker with low curvature and has an extended solid/electrolyte interphase layer, whereas the tortuous Type II consists of lithium hydride instead of lithium metal (Fig. 8B). It was known that SEI formation due to electrolyte decomposition can greatly affect the deposition morphology of Li [98,99]. However, the detailed understanding of SEI nanostructure and crystallography was not clear before development of cryo-TEM research on Li metal. In this regard many works have utilized cryo-TEM to study SEI formation on the Li electrodes that are in contact with different electrolytes/additives [93,100,101]. Fig. 8C shows that the mosaic-type SEI formed in EC/DEC electrolyte is different from the multilayer SEI formed in EC/DEC +10% FEC additive forming a layer of Li₂O at the very top SEI surface (Fig. 8D) [93]. Also, the effect of additives such as LiNO₃, as well as environmental conditions such as temperature were studied on the SEI structure [102,103]. It is concluded that the multilayer SEI maintains mechanical stability over longer cycling periods and effectively passivates the surface of deposited Li [104], while allows for uniform stripping of Li through its structure (Fig. 8E) [105].

In sum, the results suggest that electrolyte degradation, SEI formation, dendrite growth modes, and interfacial reactions are closely correlated and play synergetic role in the battery performance. A combination of cryo-EM and *in-situ* TEM should be utilized to enable *in-situ* studies of the Li deposition in different environments/conditions. Understanding the unknown formation mechanism of different SEI can greatly help in rationally designing strategies to suppress dendrites.

3.3. In-situ/Operando scanning probe-based imaging techniques: Atomic force microscopy

Atomic force microscopy (AFM) uses a micro/nano-level probe tip that provides a 3D/2D topographic image from the surface. AFM is a less explored tool for *in-situ* imaging of batteries being capable of revealing unique surface characteristics of Li microstructures. Among the benefits of AFM over other microscopy techniques is the simpler sample preparation and pretreatments. Also, it allows for experiments to be conducted in both liquid and air environments. Combination of AFM with spectroscopic techniques can provide interfacial properties in addition to the reaction kinetics. *In-situ* electrochemical (EC)-AFM that is a modified scanning probe microscopy (SPM), is suitable for electrochemical measurements, and can play a unique role in the investigation of Li metal anodes and the mechanical integrity of SEI, as well [107, 108].

Cohen et al. [109] studied the effect of solution composition, extended storage, Li deposition, and dissolution at low and high current densities on the morphology of lithium electrodes by *in-situ* AFM. They utilized variety of alkyl carbonate solutions with different salts and observed different surface morphologies under prolonged storage of Li, which were associated to different types of SEI by changing the Li salts. The non-uniformities observed in nano and micro scales cause localized deposition and stripping at parts of the SEI that have a higher

ion-conductivity. The higher conductivity can come from varying local thickness or composition in the electrolyte. The breakdown and repair of SEI film during Li dissolution was also suggested as a result of low mechanical stability of the SEI species such as ROCO2Li, Li2CO3, LiF, etc. The cracks in SEI become the preferred locations for the Li ion reduction, and locally amplified dendritic deposition of Li occurs in these spots (Fig. 9A). Fracture and continued formation of the SEI lead to consumption of both lithium and electrolyte, and increases the interfacial impedance and growth of dendrites, which leads to poor performance of Li metal anode. The mentioned characteristics are shown to be amplified upon applying higher current densities [109]. A mechanical analysis was used to study the strain-induced elastic buckling of Li thin film on a soft Polydimethylsiloxane (PDMS) substrate to determine the plane strain modulus of the SEI in different electrolytes [110]. A combination of AFM and membrane-bulge configuration has been used recently to accurately measure the stress-strain behavior of SEI [111]. Fig. 9B presents detailed surface topographies of SEI formed in EC electrolyte near the elastic limit [111]. Fig. 9B top left shows the AFM image of the SEI at a strain of \sim 3.6%. By increasing the strain to \sim 4.0% isolated cracks start to show up along longitudinal direction (determined by boxes), which further develops into complex 2D pattern by increasing the strain to 4.6% and 5.6% in Fig. 9B.

Kitta et al. [108] observed the initiation of Li deposition under operando conditions utilizing peak force tapping (PFT) mode of AFM developed by Bruker. In this scanning mode, collection of force curves from all the scan pixels allows the fast acquisition of surface images with low sample damage. Topographic height images (Fig. 9C top row) and adhesion mapping images (Fig. 9C bottom row) obtained in operando conditions, show slight contrast on the surface of the growing Li protrusions that are correlated to the preferred deposition of Li on the surface non-homogeneities. The protrusions labeled with blue arrows grew noticeably larger than the ones indicated with red arrows. The adhesion images (Fig. 9C bottom row) show higher contrast (darker) for the protrusions marked with blue arrows, indicating the small adhesion of the well-grown bumps. They correlated this observation to the varying thickness of SEI (Fig. 9D top row). Newly grown Li protrusions with thin SEI, have a low adhesion and can grow faster and the film that remains thin during growth, while a thick SEI with low Li ion conductivity prevents further growth of protrusions. Under open circuit condition (OCP), the SEI layer thickens without further growth of Li bumps (Fig. 9D bottom row).

In addition, the effect of different Li dendrite suppressive strategies such as use of additives [112,113] and surface modifications like in-situ [114] and ex-situ [115] surface film coating and nano-patterning [116] have been studied by in-situ AFM. Nano-patterning the Li surface has shown to change the surface tendency to form Li dendrites by changing the mechanical properties of the Li surface [116]. The work-hardened Li surface accommodates significant residual stress that could inhibit the formation of new high-activity sites favorable to the dendrite formation. It is shown that additives like FEC can form a compact and stiff SEI with 80% higher elastic modulus that is capable of suppressing Li dendrites [111,113]. A thin (3–4 nm) film formed during the *in-situ* experiment on Li metal as a result of pre-charging retreatment has shown to lessen the severe corrosion of Li during cycling [114]. These studies show that AFM can be used as a robust diagnostic tool to design electrolytes with stable SEI over cycling. However, the utilization of in-situ AFM imaging for the study of Li dendrites has some drawbacks. For instance, the slow imaging rate (~10 min/image) of conventional AFM technique is not suitable to record the growth process of Li dendrites when a high current density is applied. Another limitation of EC-AFM is the requirement of open-cell utilization, which makes it challenging to study Li dendrites in volatile electrolytes.

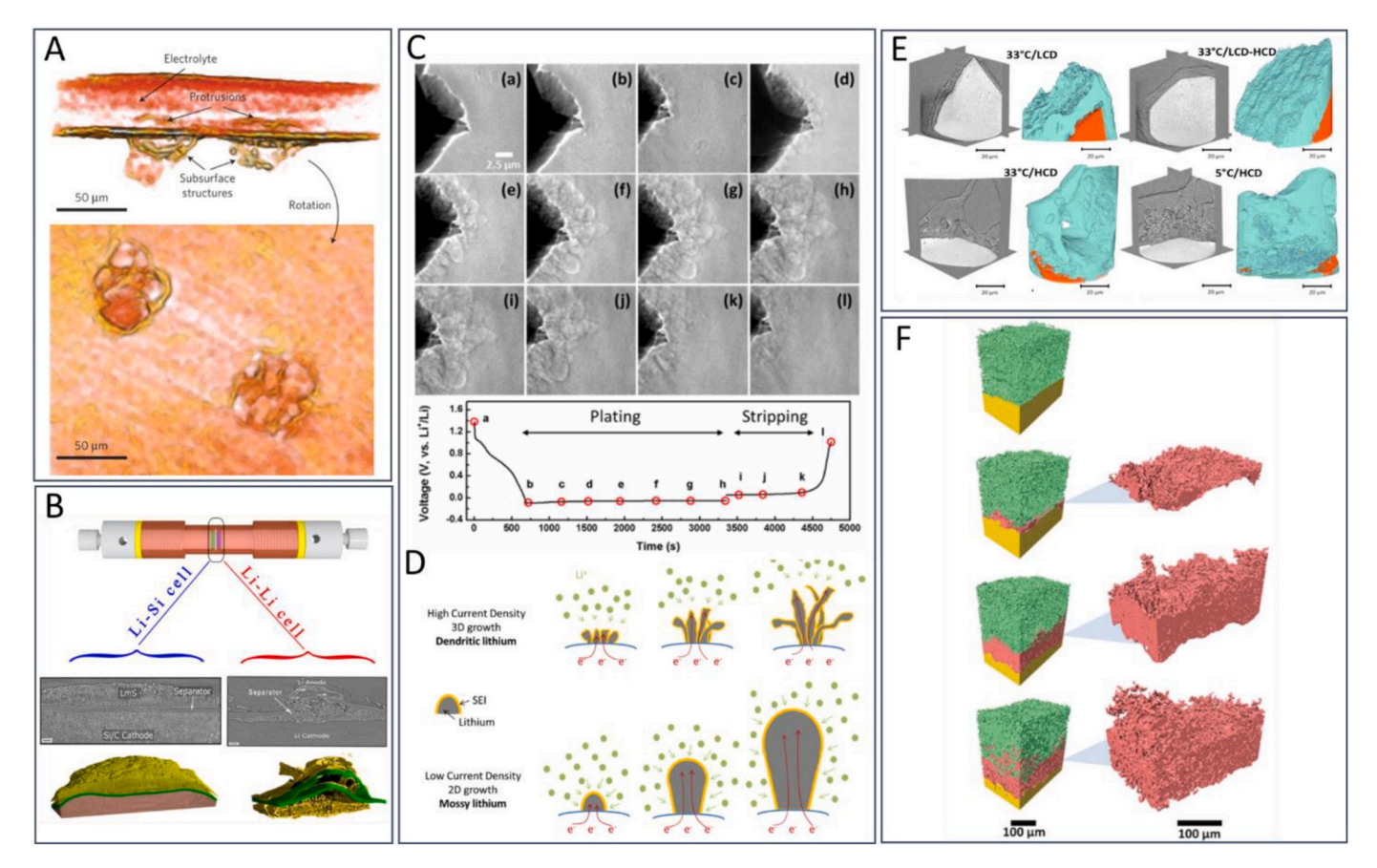


Fig. 10. Representative figures of *in-situ/operando* X-ray imaging results on Li dendrite growth. (a) Computed hard x-ray microtomography images demonstrating two adjacent dendrites and their subsurface structures: Reproduced with permission [121], Copyright 2013, Springer Nature; (b) Synchrotron x-ray phase contrast imaging results from Li–Si and Li–Li cells demonstrating the exacerbated non-uniformity of Li microstructures when cycled in half cells: Reproduced with permission [124]. Copyright 2016, American Chemical Society; (c) Visualization of Li dendrite formation and dissolution over plating and stripping electrochemical cycling processes imagedby operando transmission x-ray microscopy: Reproduced with permission [126]. Copyright 2017, American Chemical Society; (d) Schematic of narrow 3D dendritic and thick 2D mossy lithium growth formed at high and low current density, respectively: Reproduced with permission [122]. Copyright 2016, American Chemical Society; (e) Orthogonal virtual slices and corresponding segmented volume from x-ray computed tomography imaging of Li-metals cycled at low and high current density (top row) and in various temperatures (bottom row). The results demonstrate that cycling Li-metal at low current density and room temperature results in the most uniform morphology. *In-Situ/Operando* Neutron-Based Imaging Techniques: Reproduced with permission [128]. Copyright 2017, American Chemical Society; (f) Corresponding 3D visualizations of the Li surface evolution and thickening of dead Li layer over different cycle numbers: Reproduced with permission [123]. Copyright 2017, Royal Society of Chemistry.

3.4. In-situ/Operando X-ray-based imaging techniques: (Scanning) transmission X-ray microscopy/Tomography

Transmission X-ray microscopy (TXM), provides a non-destructive approach in studying the microstructural evolution of electrodeposited Li under in-situ/operando conditions. The X-ray microscopy experiments can be carried out both by a laboratory source X-ray beam and a conventional diffractometer as well as using synchrotron facilities. Using conventional laboratory X-ray systems is less costly and relatively easier. However, the synchrotron sources provide a much higher X-ray flux that improves the contrast, which is especially critical for detecting low density materials (e.g. Li) and achieving high temporal resolution. Synchrotron TXM, is a non-invasive analysis method that can detect light elements such as Li. Also, due to the high energy of hard X-rays, TXM can analyze thick samples and thus enables the analysis of commercial and packaged battery cells. X-ray microscopy can also be carried out in scanning mode (STXM), where images are recorded using a focused X-ray probe that scans the surface of specimen. In addition, construction of 3D images can be carried out utilizing computed tomography on a revolving sample during TXM imaging. The word "tomography" is composed of Greek words "tomos" meaning section and "graph", which translates to image. As such, this technique provides 3D image of an object by illuminating the sample with a penetrating beam

from various directions [117]. Additionally, *in-situ/operando* studies of Li microstructural evolution regarded as 4D X-ray tomography imaging (time added as the 4th dimension) has been performed [34,35, 118–120].

This technique was initially utilized by Harry et al. [121] to study the Li dendrite formation in symmetric cells with polymer electrolytes. Synchrotron hard X-ray microtomography that enable imaging of the structures existing on both sides of the Li electrode revealed new aspects of Li dendrite formation mechanism. This ground-breaking research demonstrated that Li dendrite formation initiates on pre-existing subsurface structures. These subsurface structures or impurities that can be found in the pre-cycled Li foils were identified as the nucleation points for Li dendrites that protrude through the separator/solid electrolyte and cause the short-circuit of the battery (Fig. 10A) [121]. Later on, Kapton capillary cells with symmetric Li electrodes were used for in-situ imaging of Li microstructure evolution in liquid electrolytes [122]. Using such novel design, formation of high surface area structures during Li deposition with a different composition compared to the metallic Li was detected through phase contrast imaging [122]. Moreover, it was demonstrated that Li stripping and redepositing processes result in the formation of cavities [123] and regrowth of Li microstructures (LmSs) that do not participate in the subsequent cycles [124, 125]. The X-ray tomography results by Sun et al. [124] demonstrated

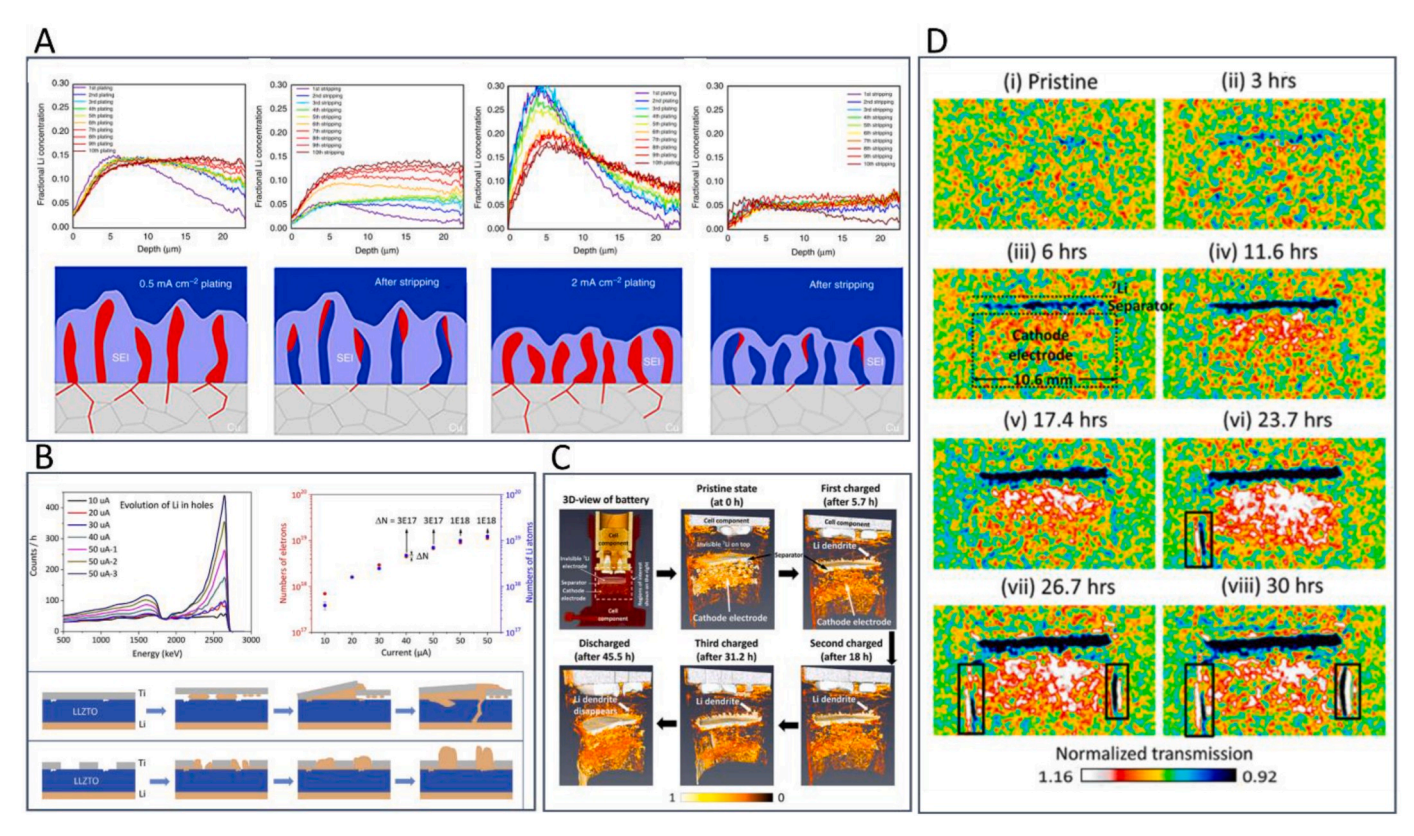


Fig. 11. Representative figures of *in-situ/operando* neutron-based imaging results on Li dendrite growth. (a) Fractional Li density from operando NDP during plating and stripping at 0.5 and 2.0 mA cm⁻² (top row) and the corresponding schematic representation of the plating and stripping process at two different current densities (bottom row) showing more nucleation points and shorter dendrites formed at higher current density: Reproduced with permission [141]. Copyright 2018, Springer Nature; (b) NDP spectra of ³H and ⁴He showing the evolution of Li in the surface holes (top row) and the corresponding schematic illustration of lithium plating under Ti film with and without holes showing the beneficial effect of 3D structures in the formation of more smooth Li deposition: Reproduced with permission [144]. Copyright 2019, Elsevier; (c) 3D evolution of the Li distribution in the battery cell at different stages of charging and discharging showing the dendritic Li growing during charge and vanishing at the end of discharge: Reproduced with permission [140]. Copyright 2019, American Chemical Society. (d) 2D evolution of Li dendrites: Reproduced with permission [140]. Copyright 2019, American Chemical Society. (For interpretation of the references to color in this figure legend, the reader is referred to the Web version of this article.)

that after the initial cycle and formation of LmSs, the further stripping of Li occurs from the metallic Li and the nascent LmSs do not show further electrochemical activity (Fig. 10B). These leads to gradual consumption of Li metal and formation of inactive/dead Li compounds that eventually protrude through the solid electrolyte and cause short circuit and catastrophic failure of the battery cells [124,125]. It was also demonstrated that the failure mechanism of symmetric Li/Li cells is rapid and more severe compared to the Li/Si(C) systems [124]. Additionally, time laps laboratory X-ray tomography demonstrated the formation and gradual penetration of moss-like Li deposits into the separator, which indicates the importance of separator properties such as tortuosity when used in Li metal batteries [123]. Cheng et al. [126] utilized operando 2D TXM to investigate the Li deposition behavior and understand the effect of current density on Li microstructure (Fig. 10C). High resolution TXM results that distinct between the mossy and dendritic Li microstructures, demonstrated the preferred dendrite formation under high current Li deposition, leading to increased dead Li formation (Fig. 10D). Additionally, X-ray imaging was utilized to study the effect of temperature on the Li microstructural evolution [127,128], which showed that lower temperatures induces more voids and increases the surface area of Li microstructures (Fig. 10E) [127,128]. Microstructural evolution of deposited Li metal during prolonged cycling condition was also studied using time lapsed laboratory X-ray CT imaging. This work demonstrated the formation of a mossy-like Li microstructure which penetrated through the separator gradually through repeated cycles of plating and stripping (Fig. 10F) [123]. Recently, Kasemchainan et al. [129] utilized

in-situ X-ray CT imaging to identify a critical stripping current density that results in formation of Li dendrites on plating. Dendrite formation was suggested to be the result of higher rate of Li removal from bulk Li electrode than that of replenished that leads to formation of voids, which act as hot spots for Li dendrite formation.

In conclusion, X-ray tomography and imaging are popular techniques for the direct study of Li microstructural evolution. They provide valuable insights about the degradation and failure mechanisms of Li metal batteries [125], and allow for optimization of cell parameters such as current density [127], temperature [128], choice of electrolyte and separator [130–132].

3.5. In-situ/Operando neutron-based imaging techniques: Neutron depth profiling and radiography/tomography

Neutron imaging results have so much in common with X-ray images; however, neutrons have a stronger attenuation compared with X-rays when interacting with light elements such as Li [133]. When a neutron beam passes through a Li-containing sample, the neutrons react with the $^6\mathrm{Li}$ isotope and generate two charged particles with well-defined energies ($^4\mathrm{He}$ (2044 keV) and $^3\mathrm{H}$ (2727 keV)) that lose their energy at a known rate when travelling through the cross section of the sample. Based on their energy loss and the stopping power of the material, original position of $^6\mathrm{Li}$ through the cross section of the sample can be identified. So, neutron depth profiling (NDP) allows for direct quantification of lithium concentration as a function of sample depth.

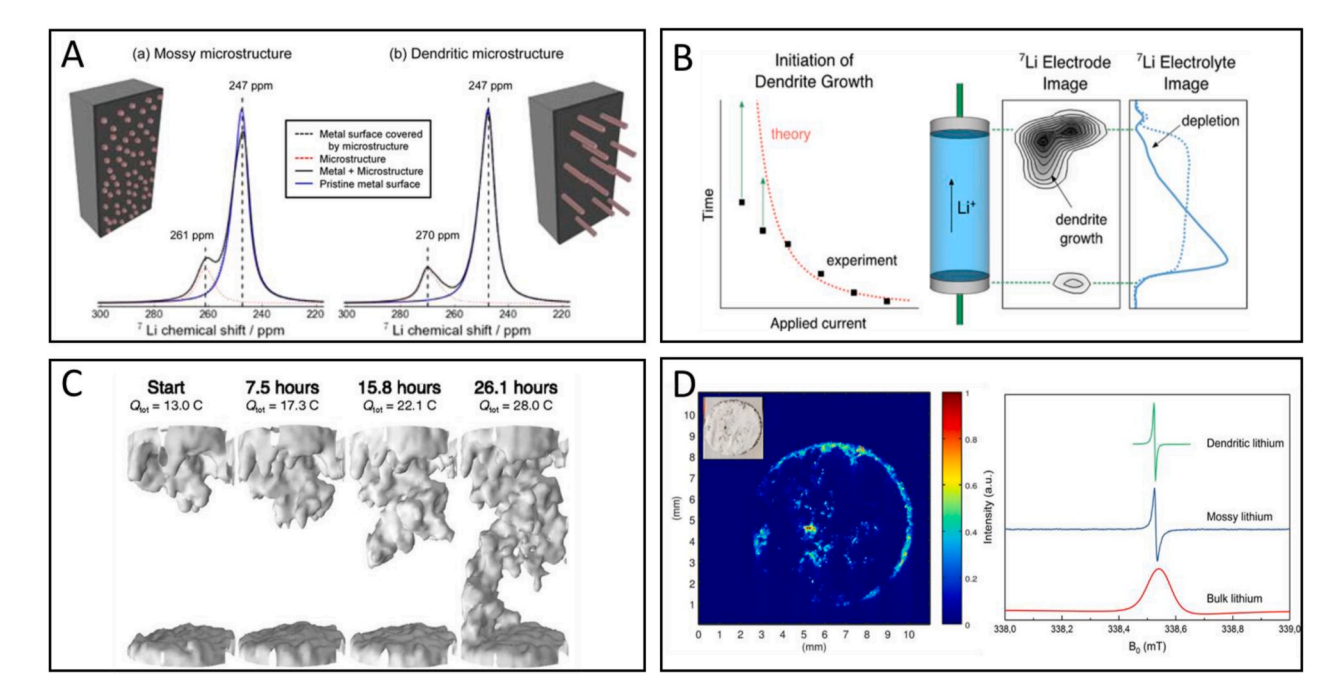


Fig. 12. Representative figures of *in-situ/operando* resonance-based imaging results on Li dendrite growth. (a) Change of Li NMR spectra in the case of mossy and dendritic microstructures deposition showing the peak shift from 261 to 247 ppm by changing the Li microstructure from mossy to dendritic, respectively: Reproduced with permission [21]. Copyright 2015, American Chemical Society; (b) Plot of the theoretical Sand's time and the experimentally measured initiation time of dendrite growth (left) and the MRI signal showing the evolution of the ⁷Li electrolyte concentration profile and the corresponding ⁷Li chemical shift image of the Li metal electrode showing the initiation of Li dendrites(right): Reproduced with permission [157]. Copyright 2015, American Chemical Society; (c) 3D high resolution reconstruction of lithium dendrite microstructure by the dendrites' indirect MRI imaging of the surrounding electrolyte overtime resulting in a short circuit between electrodes: Reproduced with permission [158]. Copyright 2016, National Academy of Sciences; (d) EPR image of lithium dendrites grown inside a glass fiber separator (left) and First derivative CEPR signal, as measured in a field swept EPR experiment, for metallic lithium with different morphologies ranging from bulk, mossy and dendritic structures: Reproduced with permission [134]. Copyright 2018, Springer Nature.

Knowing that each generated particle represents one Li, NDP can measure the Li density with high sensitivity as a function of depth. This non-destructive analysis method can be used to identify the location of electrochemical reactions in battery cells, Li dendrite formation mechanism, interfacial transport behavior and kinetics of Li transport, quantifying the density of the Li dendrites and assessing the reversibility of electrochemical reactions with temporal resolution of ~ 30 s and depth resolution of ~ 70 nm in *operando* conditions [134–136].

In-situ neutron diffraction was first utilized to distinguish the onset of Li plating on graphite anode [137]. The increase in the LiC₆ (the phase with the highest Li level) peak intensity is the indicator of Li plating on the graphite surface at the end of charge. NDP was used to reveal the Li plating/stripping behavior at the interface of liquid or solid electrolytes with metallic Li, achieved by direct measurment of the Li-ion concentration profiles [138-140]. The short-circuit prediction capability of in-situ NDP measurement was demonstrated according to the increasing NDP count prior to short-circuiting [138]. This technique was also used as a complementary to microscopy techniques, providing the spatial density of lithium during plating/stripping [140,141]. It was also shown that Li plating dramatically increases above a threshold current of C/2 at a temperature of -2 °C [142]. Recently, Lv et al. [141] showed that the density of the initially forming Li-metal strongly depends on the applied current density and its morphology templates the concurrently forming SEI. Fig. 11A shows the Li density profiles after each plating and stripping cycle at two different current densities of 0.5 and 2 mA cm⁻². The top row panels in Fig. 11A indicates denser Li plating for the current density of 2 mA cm⁻². The less dense Li plating at low current density results in thicker SEI formation and consequently more amount of "dead" Li, which is schematically depicted for better understanding in Fig. 11A bottom row. It should be realized that the total amount of inactive Li quantified by NDP is a combination of both dead Li metal and the Li ions existing in the SEI. It is worth noting that a limited

penetration of Li into the Cu current collector was detected (20 µg cm⁻²), which is partially reversible (4 µg cm⁻² remains after stripping). Noteworthy, the early stages of Li penetration through current collector has been visualized by means of *in-situ* SEM, as well [77]. Additionally, NDP allows for visualization of the direct deposition of Li inside solid electrolytes [138,143]. Li et al. [144] captured the lithium plating behavior at the interface of Li_{6.4}La₃Zr_{1.4}Ta_{0.6}O₁₂ (LLZTO) solid electrolyte and 3D/2D Ti current collector. Knowing that the kinetic energy of the Li particles travelling through Ti layer attenuates much more than those through holes, the stopping power of ⁴He at Ti film is large enough to distinguish between the increasing lithium atoms under 2D Ti film and in the holes present in the 3D Ti. This work demonstrated the preferred deposition of Li in the void spaces of 3D Ti electrode, which greatly diminish solid electrolyte/electrode interface degradation and validates the positive impact of a structured 3D electrode on Li deposition uniformity. From these understandings the possible model for the lithium plating in the flat and hole-containing battery systems is proposed (Fig. 11B). Recently, Han et al. [145] highlighted that partial electronic conductivity of solid electrolytes especially in the grain boundaries can initiate the Li deposition and penetration even in disconnected pores. Electrons can combine with Li ions at the grain boundary, reduce Li-ions between the solid electrolyte grains and eventually cause short circuit in the battery.

Although, NPD is robust technique to depth profiling of Li concentration, it does not allow for direct visualization of Li metal microstructures. However, neutron radiographic imaging (NRI), is capable of imaging the Li microstructures based on the level of neutron absorption and penetration in various areas of the sample depending on its density and composition [146]. Song et al. [140] for the first time performed 3D tomography high-resolution *operando* neutron scattering studies and visualized branch-like Li dendrites with progressive growth at different stages of charging (Fig. 11C). The dynamic features were also revealed

through 2D *operando* radiography during charging period showing increased depletion of Li over time (Fig. 11D). They also investigated the Li dendrite short-circuit and post shorting effects to understand the thermal runaway as a result of Li dendrites.

Overall, although neutron-based profiling and imaging can provide unique and valuable information regarding Li metal batteries, there are several constraints associated with utilizing such techniques. For instance, the generation and handling of a neutron probe in the laboratory scale is more challenging and time consuming in comparison to X-rays and electron beams. Also, having smooth surfaces/interfaces for neutron imaging is highly necessary, and an intense volume change during Li deposition can lead to artifacts and inaccurate NRI and NDP results. Additionally, natural lithium consists of only 7.5% ⁶Li, thus a better noise-to-signal ratio can be obtained on a ⁶Li enriched battery, which increases the complexity of the experiments. Also, because the created alpha and tritons particles will strongly get absorbed by metals, very thin current collector and no metallic casing is desired for NDP and NRI experiments.

3.6. In-situ/Operando resonance-based imaging techniques

3.6.1. Nuclear magnetic resonance (NMR)

Nuclear magnetic resonance (NMR) is able to detect the local magnetic fields around atomic nuclei, and allows the detection and monitoring of the microstructural evolution of Li metal during depositing and stripping processes. This is because the resonance from Li in diamagnetic structures such as electrolyte and the SEI is well separated from the resonance from paramagnetic Li metal, which is shifted to about 260 ppm, by the Knight Shift mechanism [147]. In other words, slight shift in the NMR signal frequencies can provide detailed information about the local electronic environment of 7Li and 6Li around the nucleus and electrochemically induced structural changes of the Li metal electrodes. NMR is a quantitative analysis technique, but due to inability to use magic angle spinning, it lacks high spatial resolution (resolution is limited to \sim 15–25 μ m). However, NMR has shown a great potential in measuring the Li-ion concentration gradient [148] and also monitoring Li dendrite formation [21]. Penetration depth of radiofrequency (RF) signal to the bulk of Li metal is limited to $< 15 \mu m$ (known as skin effect), and it is known that the feature size of Li microstructures (moss and dendrites) are smaller than 15 μm . Thus, in a constant mass of Li in a symmetric cell, a change in the extent of $^7\mathrm{Li}\ \mathrm{NMR}$ signal corresponds to a change in the surface/bulk fraction of Li metals [149]. Therefore, ⁷Li NMR provides a direct way to monitor the formation of Li microstructures with <15 μm feature size [150,151]. Noteworthy, ⁷Li NMR allows for quantified analysis of Li microstructural evolution, whereas quantified information is not achievable through other imaging techniques.

Using such potent technique, Bhattacharyya et al. [8] were able to quantify the microstructural evolution of electrochemically deposited Li in symmetric cells cycled with different electrolytes. Due to the skin effect and the subsurface penetration of RF-field, the NMR signal is proportional to the area of the Li microstructure, thus can monitor and quantify the evolution of Li microstructure formed during plating/stripping. Later on, using in-situ NMR results corroborated with SEM imaging it was demonstrated that formation of different Li microstructures results in a change in the Li chemical shift [21]. Specifically, formation of thick and dendritic Li microstructures gives rise to an additional NMR peak at higher frequency region of the spectrum, which can help in distinguishing between mossy and dendritic deposition of Li (Fig. 12A). Intensity of the NMR peaks define the amount of material, while the chemical shifts show formation of different compounds. Therefore rapid and quantified analysis of the microstructural evolution of Li as a function of cell pressure [21], temperature regimes [149] and electrolyte compositions [8] were carried out using NMR. Using 1D NMR imaging Klamor et al. [152] could determine the concentration profile of the anions and correlate the Li⁺ accumulation near the electrode surface to the formation of SEI. However, one main limitation of NMR is that its spatial resolution is limited to about 50 µm, while the expected thickness of the SEI is only a few tens of nanometers [153]. Therefore, dynamic nuclear polarization (DNP) in which the large polarization of unpaired electrons is conveyed to nearby coupled nuclear spins by microwave, have been incorporated to increase the sensitivity of NMR to study thin SEI layers [154]. However, in typical DNP experiments, a solution with organic radicals are added to the electrolyte that can increase the level of impurities and induce artifact to the SEI composition. In addition, it requires cooling the sample to cryogenic temperatures, which eliminates the chance of in-situ studies. Very recently, Hope et al. [155], utilized the inherent conduction electrons to hyperpolarize the room temperature ⁷Li NMR signal of Li metal with higher magnetic field and microwave source under magic angle spinning (MAS) to study SEI. This recent development indicates the possibility of utilizing high resolution NMR for in-situ studies of SEI and Li dendrite formation.

3.6.2. Magnetic resonance imaging (MRI)

Although NMR provides valuable quantitative information about the microstructural evolution of Li metal, it cannot image the morphology and shape of the Li microstructures. However, magnetic resonance imaging (MRI) that is a resonance based, non-invasive diagnostic tool can address this issue by providing spatially resolved ⁷Li MRI chemical shift images (CSI). The orientation of Li metal microstructures with respect to the external magnetic field (B₀), can result in the chemical shift in the NMR spectra. Since the Li dendrites generally grow perpendicular to the bulk Li metal electrodes, one can distinguish the signal from Li dendrites from that of the Li electrode. CSI demonstrated the Li microstructures with a resolution of 60 $\mu m \times 376 \mu m$ [156]. The spatial resolved information revealed that the dendritic Li have a narrow range of chemical shifts near 270 ppm in contrast to the broad peak of mossy microstructures in the range of 262-274 ppm. Moreover, through 2D in-situ CSI the sequence of Li microstructure evolution from mossy to dendritic was investigated under various current rates [157]. It was experimentally demonstrated that at high current rates the Li dendrite formation is a function of Li depletion at the electrolyte (Fig. 12B), which is close to Sand's time theory. At low current rates, Li dendrites start to grow at earlier stages than predicted theoretically (Fig. 12B left), which denotes to a different and elusive mechanism for dendrite formation at low current regime [157]. It was further demonstrated that dendrites could be imaged indirectly by fast ¹H MRI method. This imaging method that is based on the changes in Li concentration, allows for imaging the Li depletion regions, has a poor spatial resolution and only identifies the shadow of dendrites (space taken up by the dendrites). Fig. 12C shows the series of 3D MRI images, which depicts the evolution of the deposited Li morphology over time [158]. Li-metal deposition behavior can also be predicted by analyzing the evolution of electrolyte due to high concentration of Li-ions, narrow line widths, and accepted signal lifetimes [159]. As such, in-situ MRI has been used in solid electrolytes such as Li₁₀GeP₂S₁₂, where Li inhomohenity and local depletion of electrolyte in Li/solid electrolyte interface were identified [160]. In addition Li microstructural growth and short-circuit through solid electrolyte were recently detected in the garnet-type solid electrolyte, Li_{6.5}La₃Zr_{1.5}-Ta_{0.5}O₁₂, through ⁷Li NMR/MIR imaging [161]. However, it should be noted that the short-circuit events cuased by dendrites smaller than the detection limit of the NMR measurements, cannot be detected. Noteworthy, although most of the MRI studies were performed in the specifically made cells, "inside-out" MRI technique has enabled studying the electrode materials in commercial cell designs without requiring RF access to the inside of the cell [162]. This is because, the magnetic field produced by the cell is material dependent and varies over change in materials distribution during cell operation.

3.6.3. Electron paramagnetic resonance (EPR)

Electron Paramagnetic Resonance (EPR) allows for studying materials with unpaired electrons and utilizes a similar concept to NMR.

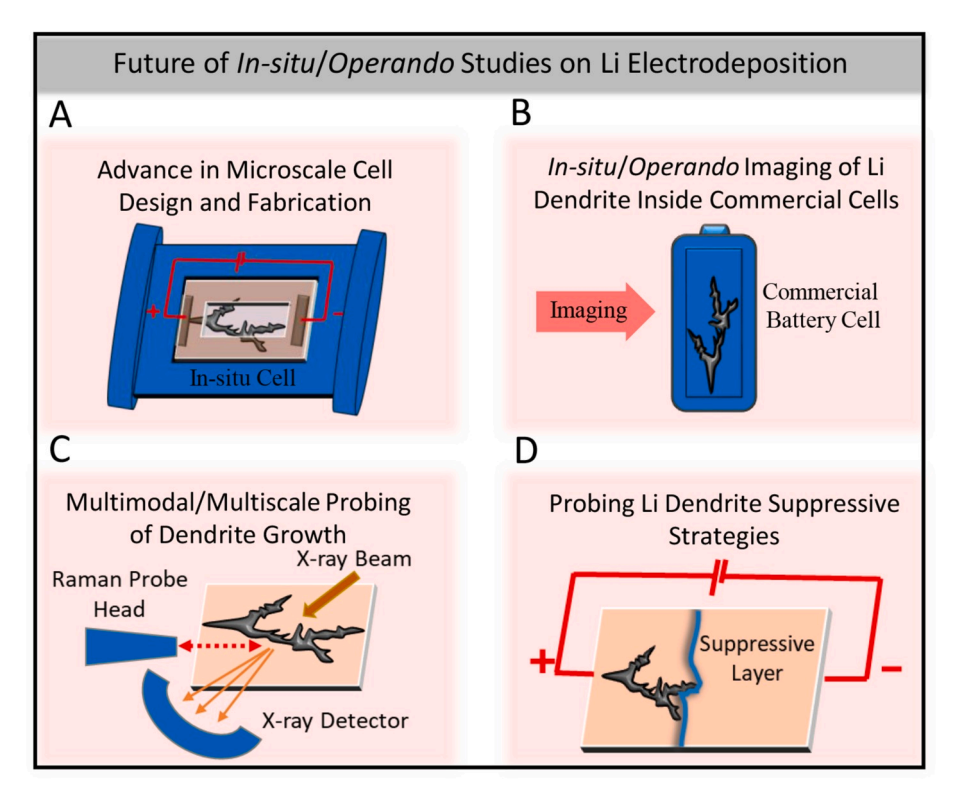


Fig. 13. Future of *in-situ/operando* studies on Li electrodeposition in batteries. (a) Design of advanced in-situ cells being close to the real-life cell models with low introduction of artifacts; (b) Imaging of Li dendrites formed inside real-life battery cells; (c) Simultaneous multimodal and multiscale study of Li dendrites; (d) Probing the mechanisms of the mitigating strategies proposed for Li dendrites growth.

However, despite the NMR where the spins of atomic nuclei are recorded, EPR relies on the detection of electron spins. Therefore, EPR requires a higher electromagnetic frequency compared to that of NMR in the same magnetic field strength. Thus, EPR utilizes microwaves instead of radio waves used in NMR experiments. This leads to ~10 times smaller skin depth than NMR, making it highly sensitive to thin surface layer of the Li microstructures based on the signal width [163-166]. Noteworthy the penetration depth of microwave field in metallic Li is much smaller than RF signal, limiting the skin depth effect to about 1.1 μm for Li, which results in more sensitive analysis of Li microstructure localization [165,166]. Although, EPR can achieve better spatial resolution (about 8 µm), which is highly superior to the spatial resolution achieved by MRI (>100 μm) [164], majority of its application has been limited to biology and was not largely utilized in studying battery systems. This is mainly due to the cell design constrains such as compatibility, transparency to microwave radiation and EPR inactivity of the electrochemical cells [167]. The Li EPR signal depends heavily on concentration of impurities and disorder in Li structure, which leads to featureless spectrum from the bare Li metal foil and high selectivity for dendrite detection [167]. The peaks ascribed to Li microstructures can be utilized for electron paramagnetic resonance imaging (EPRI), which enables the monitoring of Li dendrite localization during operando measurements by implementing novel cell designs (Fig. 12D) [163,164]. Finally EPR imaging can be considered as another unique and semi-quantitative tool in studying and optimizing the electrochemical cell variables to achieve uniform and non-dendritic Li metal deposition [168].

4. Conclusion and outlook

Understanding the fundamentals of dendrite nucleation and growth is critical for developing strategies to prevent/suppress dendritic Li deposition for viable Li metal batteries. For a long time Chazalviel's space charge theoretical calculations and its derivatives were the only

models explaining the dendritic deposition of Li in dilute electrolytes. Understanding the mechanism behind the notorious behavior of Li deposition has always been challenging through experimental works and in real life battery conditions. This is mainly due to the high reactivity and sensitivity of Li metal and the misleading effects of experimental conditions on its structure and morphology. The recent technological advancements in materials characterization techniques and development of sophisticated cell design for various in-situ/operando imaging techniques have offered novel understandings on morphological, structural and chemical characteristics of the Li dendrites. In this work, we reviewed the technical aspects of in-situ/operando imaging studies on the Li dendrite deposition behavior and discussed the achieved scientific understandings. These techniques include optical imaging, electron microscopy, scanning probe imaging, X-ray microscopy, neutron and resonance-based imaging approaches. Such in-situ/operando imaging techniques are designed to minimize the exposure of highly sensitive Li metal to air/moisture, restrict beam damage and reduce post-mortem experimental artifacts.

Optical microscopy is a simple and reliable *operando* imaging tool with high temporal resolution, for which the cells can be built easily with glass slides/cuvettes; however, the spatial resolution is poor, being limited by the wavelength of light (200 nm). No analytical information can be obtained through optical microscopy technique; although, complementary to optical microscopy, Raman imaging can provide information about the spatial distribution of chemical compounds in the sample and can identify the variation in Li-ion concentration at the Li/electrolyte interface. However, it has a lower temporal resolution as the existence of electrolyte and surface deposits weakens the Raman signal and adds artifacts to data interpretation.

Electron microscopy has very high spatial resolution compared to optical microscopy (e.g. 2–10 nm for SEM and 0.2–0.05 nm for TEM), capable of revealing the microstructures of Li dendrites and the SEI at the early stages of formation. However, electron microscopy has its own drawbacks, e.g. significant beam damage, ultra-high vacuum operation

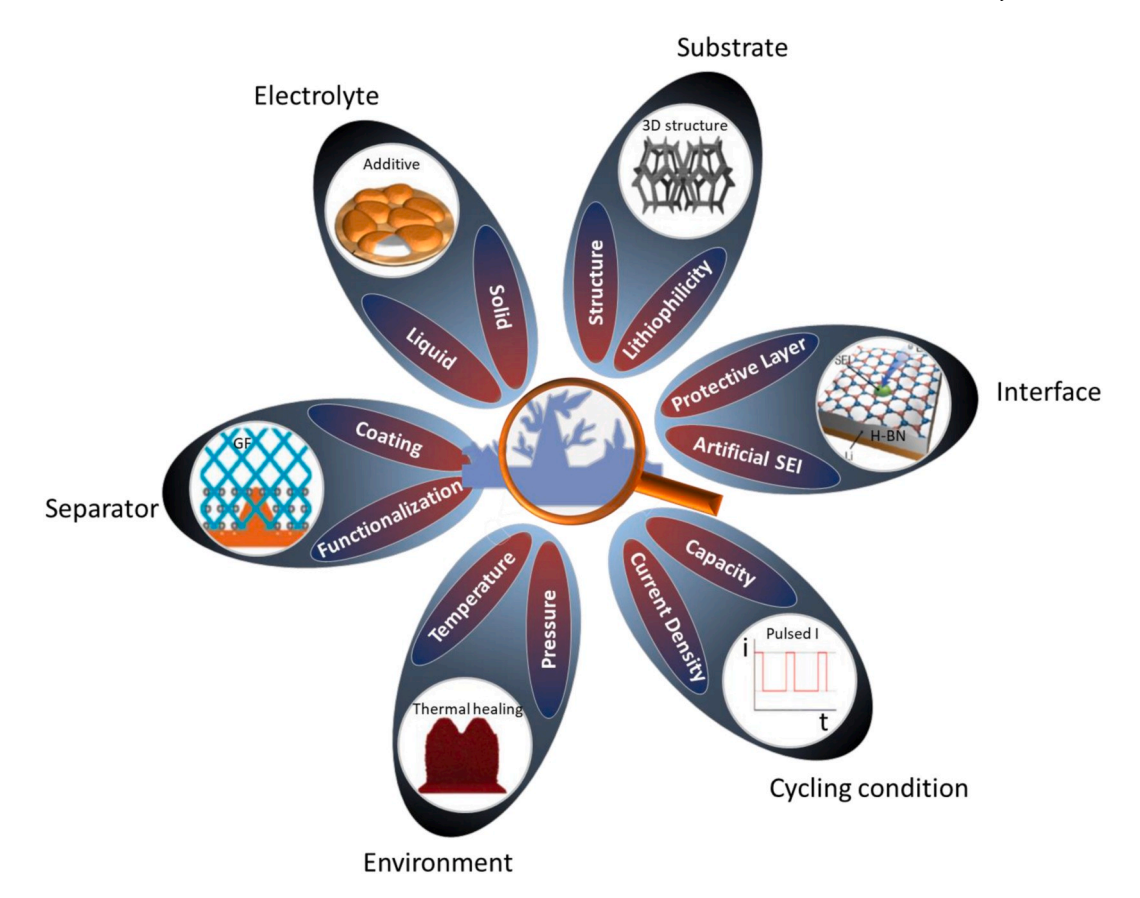


Fig. 14. Different parameters shown to be effective in suppression of Li dendrites that need to be visited by *in-situ/operando* imaging techniques to develop an effective mitigation strategies: Reproduced with permission [98,173–177]. Copyright 2015, Springer Nature. Copyright 2018, The American Association for the Advancement of Science. Copyright 2014, American Chemical Society. Copyright 2017, American Association for the Advancement of Science. Copyright 2016, John Wiley and Sons. Copyright 2019, American Chemical Society.

environment and complicated design of In-situ/operando beamtransparent liquid-cells, which limit the achievable spatial resolution. The integration of fast direct electron detection cameras and enhancement of cell designs are critical for high resolution imaging of Li dendrites in such environment. Recently, cryo-TEM studies showed major contributions to resolving the nanostructure and crystallographic details of Li and SEI at high spatial resolutions. The cryo-TEM results are very reliable as the beam damage is highly controlled and also the samples can be preserved at their natural state. However, cryo condition does not allow for in-operando imaging of Li dendrites during nucleation and growth. The freezing processes are mainly developed for biological samples with low thickness, which is challenging in Li electrodeposition studies. Considering the sensitivity of Li to the electron beam, directdetection electron-counting cameras with high quantum efficiencies are needed to record images at high frame rates [169]. Designing the experimental parameters is also challenging. For instance, conventional wisdom suggests that a lower voltage TEM (<100 keV) should reduce beam damage for a metallic sample like Li. However, it is shown that higher voltage can minimize the interaction of Li with the electron beam and reduce specimen heating, radiolysis, and sputtering damage [93]. On the other hand, compared to electron-based techniques, X-ray imaging does not induce significant beam damage artifacts and can penetrate through thick samples. This enables operando/in-situ imaging of Li dendrites in solid electrolytes and also commercial cells with liquid electrolytes. However, lack of chemical information and insufficient temporal and spatial resolution is the main drawback of X-ray imaging. Neutron-based imaging, with higher sensitivity compared to X-ray imaging, can investigate the Li plating behavior inside solid electrolytes and recognize the reaction location by visualization of Li concentration profiling of Li-ions in the battery cross section. Resonance-based

imaging can distinguish between different types of Li deposition, from bulk to mossy and dendritic, and quantify the Li microstructures but does not provide very high spatial resolution. The recent improvement utilizing magic angle spinning (MAS) technology in room temperature and inside-out MRI technique, mapping the magnetic field changes surrounding the cell, show the possibility of utilizing high resolution resonance-based techniques for in-situ studies of SEI and Li dendrite formation in commercial battery cells. However, performing the in-situ electrochemical experiments under spinning conditions are challenging. AFM can provide information on the topography, mechanical and electrochemical properties of the lithium/electrolyte interface and SEI, which is shown to be among the critical parameters affecting the formation and growth of Li dendrites. It would be substantial to track the movement of single Li atoms inside SEI and along the grain boundaries and visualize the interfacial reactions in complementary to the DFT calculations [170,171].

As mentioned earlier, a critical part of <code>in-situ/operando</code> battery research is the design of electrochemical devices compatible with the applied techniques, close to the typical cell models and low possibility for artifacts (Fig. 13A). For example, electron microscopy requires thin liquid layer to be transparent to electrons for visualization of Li structures. MRI requires RF access to the inside of the cell. Also, special design is needed for 3D images in MRI and XRT to make sure the beams are not blocked during the rotation of sample. Cell designs for <code>in-situ/operando</code> imaging has continuously been revisited and improved in the past few years, but still there is a long way to image the commerical batteries <code>in operando</code> conditions and achieve a highly realistic and reliable understanding about the Li dendrites (Fig. 13B).

Another potential future direction would be to integrate multiscale characterization techniques in order to gain multidimensional

information on Li metal anode deposition (Fig. 13C). Multimodal/multiscale measurements can provide new insights and answer fundamental issues such as the significance of SEI on morphological evolution of Li metal, which drive research forward and enable innovative solutions. For example, X-ray techniques such as TXM can provide high penetration depth, important for analysis of commercial batteries. In addition, X-ray based techniques cause less beam-induced damage compared to electron microscopy, but with the cost of reduced spatial resolution. Thus, these techniques can be used complementary to each other to provide detailed and comprehensive information. As an example, a homemade bimodal Raman-TEM has already been developed in National Institute of Standards and Technology (NIST) that can provide atomic-scale dynamic imaging together with detailed chemical analysis [172].

Another prospective contribution of in-situ/operando techniques can be the evaluation and elucidation of Li electrodeposition behavior under mitigation strategies (Fig. 13D) [98,173-177]. Although there are several methods proposed to mitigate the dendritic electrodeposition of Li metal (Fig. 14), only few of such works have included in-situ and operando imaging techniques to fundamentally examine the effectiveness of their approaches. For instance, a few in-situ/opererando studies have been carried out to identify the mechanism for improved Li deposition behvior using modifed electrolytes [178], additives [78, 179], current densities [55,91], the electrodeposition substrate composition [77] and substrate morphology [116,180]. However, underlying mechanism for improved cycling stability of various engineered Li-metal batteries are not fully udnerstood. Therefore, extensive utilization of in-situ and operando imaging techniques in quest for uncovering the most effective approaches from the pool of several Li dendrite suppression strategies should be considered for future works.

Declaration of competing interest

The authors declare that they have no known competing financial interests or personal relationships that could have appeared to influence the work reported in this paper.

CRediT authorship contribution statement

Tara Foroozan: Conceptualization, Writing - original draft. **Soroosh Sharifi-Asl:** Writing - review & editing. **Reza Shahbazian-Yassar:** Supervision, Writing - review & editing.

Acknowledgments

R. Shahbazian-Yassar acknowledges the financial support from National Science Foundation (NSF) under Grand No. CBET-1805938.

References

- M.S. Whittingham, Lithium batteries and cathode materials, Chem. Rev. 104 (2004) 4271–4301.
- [2] M.S. Whittingham, Electrical energy storage and intercalation chemistry, Science 192 (1976) 1126 LP–1127 (80-.).
- [3] F. Wu, Y.X. Yuan, X.B. Cheng, Y. Bai, Y. Li, C. Wu, Q. Zhang, Perspectives for restraining harsh lithium dendrite growth: towards robust lithium metal anodes, Energy Storage Mater. 15 (2018) 148–170.
- [4] S.S. Zhang, Problem, status, and possible solutions for lithium metal anode of rechargeable batteries, ACS Appl. Energy Mater. 1 (2018) 910–920.
- [5] C. Brissot, M. Rosso, J.-N.N. Chazalviel, S. Lascaud, Dendritic growth mechanisms in lithium/polymer cells, J. Power Sources 81 (1999) 925–929.
- [6] S. Li, M. Jiang, Y. Xie, H. Xu, J. Jia, J. Li, Developing high-performance lithium metal anode in liquid electrolytes: challenges and progress, Adv. Mater. 30 (2018) 1–29.
- [7] A.N. Dey, S.E.M. studies of the Li-film growth and the voltage-delay phenomenon associated with the lithium-thionyl chloride inorganic electrolyte system, Electrochim. Acta 21 (1976) 377–382.
- [8] R. Bhattacharyya, B. Key, H. Chen, A.S. Best, A.F. Hollenkamp, C.P. Grey, In situ NMR observation of the formation of metallic lithium microstructures in lithium batteries, Nat. Mater. 9 (2010) 504–510.

- [9] K.N. Wood, E. Kazyak, A.F. Chadwick, K.-H. Chen, J.-G. Zhang, K. Thornton, N. P. Dasgupta, Dendrites and pits: untangling the complex behavior of lithium metal anodes through operando video microscopy, ACS Cent. Sci. 2 (2016) 790–801.
- [10] H. Kim, G. Jeong, Y.-U.U. Kim, J.-H.H. Kim, C.-M.M. Park, H.-J.J. Sohn, Metallic anodes for next generation secondary batteries, Chem. Soc. Rev. 42 (2013) 9011–9034
- [11] M.D. Tikekar, S. Choudhury, Z. Tu, L.A. Archer, Design principles for electrolytes and interfaces for stable lithium-metal batteries, Nat. Energy 1 (2016) 16114.
- [12] E. Peled, The electrochemical behavior of alkali and alkaline earth metals in nonaqueous battery systems—the solid electrolyte interphase model, J. Electrochem. Soc. 126 (1979) 2047–2051.
- [13] X.-B. Cheng, R. Zhang, C.-Z. Zhao, Q. Zhang, Toward safe lithium metal anode in rechargeable batteries: a review, Chem. Rev. 117 (2017) 10403–10473.
- [14] I. Yoshimatsu, T. Hirai, J. Yamaki, Lithium electrode morphology during cycling in lithium cells, J. Electrochem. Soc. 135 (1988) 2422–2427.
- [15] X. Guan, A. Wang, S. Liu, G. Li, F. Liang, Y.-W. Yang, X. Liu, Luo, J. Controlling nucleation in lithium metal anodes, Small 1801423 (2018) 1801423.
- [16] J.N. Chazalviel, Electrochemical aspects of the generation of ramified metallic electrodeposits, Phys. Rev. A 42 (1990) 7355–7367.
- [17] M. Rosso, T. Gobron, C. Brissot, J. Chazalviel, S. Lascaud, Onset of dendritic growth in lithium/polymer cells, J. Power Sources 98 (2001) 804–806.
- [18] A. Teyssot, C. Belhomme, R. Bouchet, M. Rosso, S. Lascaud, M. Armand, Interelectrode in situ concentration cartography in lithium/polymer electrolyte/ lithium cells, J. Electroanal. Chem. 584 (2005) 70–74.
- [19] C. Monroe, J. Newman, Dendrite growth in lithium/polymer systems: a propagation model for liquid electrolytes under galvanostatic conditions, J. Electrochem. Soc. 150 (2003).
- [20] C. Monroe, J. Newman, The impact of elastic deformation on deposition kinetics at lithium/polymer interfaces, J. Electrochem. Soc. 152 (2005) 396–404.
- [21] H.J. Chang, N.M. Trease, A.J. Ilott, D. Zeng, L.S. Du, A. Jerschow, C.P. Grey, Investigating Li microstructure formation on Li anodes for lithium batteries by in situ ⁶Li/⁷Li NMR and SEM, J. Phys. Chem. C 119 (2015) 16443–16451.
- [22] E.J. Cheng, A. Sharafi, J. Sakamoto, Intergranular Li metal propagation through polycrystalline Li6.25Al0.25La3Zr2O12 ceramic electrolyte, Electrochim. Acta 223 (2017) 85–91.
- [23] Y. Ren, Y. Shen, Y. Lin, C.W. Nan, Direct observation of lithium dendrites inside garnet-type lithium-ion solid electrolyte, Electrochem. Commun. 57 (2015) 27–30.
- [24] S. Yu, D.J. Siegel, Grain boundary softening: a potential mechanism for lithium metal penetration through stiff solid electrolytes, ACS Appl. Mater. Interfaces 10 (2018) 38151–38158.
- [25] C. Xu, Z. Ahmad, A. Aryanfar, V. Viswanathan, J.R. Greer, Enhanced strength and temperature dependence of mechanical properties of Li at small scales and its implications for Li metal anodes, Proc. Natl. Acad. Sci. 114 (2017) 57–61.
- [26] L. Zhang, T. Yang, C. Du, Q. Liu, Y. Tang, J. Zhao, B. Wang, T. Chen, Y. Sun, P. Jia, H. Li, L. Geng, J. Chen, H. Ye, Z. Wang, Y. Li, H. Sun, X. Li, Q. Dai, Y. Tang, Q. Peng, T. Shen, S. Zhang, T. Zhu, J. Huang, Lithium whisker growth and stress generation in an in situ atomic force microscope environmental transmission electron microscope set-up, Nat. Nanotechnol. 15 (2020).
- [27] D.R. Ely, R.E. García, Heterogeneous nucleation and growth of lithium electrodeposits on negative electrodes, J. Electrochem. Soc. 160 (2013) 662–668.
- [28] E. Peled, The electrochemical behavior of alkali and alkaline earth metals in nonaqueous battery systems—the solid electrolyte interphase model, J. Electrochem. Soc. 126 (1979) 2047.
- [29] J.B. Goodenough, Y. Kim, Challenges for rechargeable Li batteries, Chem. Mater. 22 (2010) 587–603.
- [30] A. Wang, S. Kadam, H. Li, S. Shi, Y. Qi, Review on modeling of the anode solid electrolyte interphase (SEI) for lithium-ion batteries, npj Comput. Mater. 4 (2018).
- [31] D. Aurbach, Review of selected electrode-solution interactions which determine the performance of Li and Li ion batteries, J. Power Sources 89 (2000) 206–218.
- [32] E. Peled, D. Golodnitsky, G. Ardel, Advanced model for solid electrolyte interphase electrodes in liquid and polymer electrolytes, J. Electrochem. Soc. 144 (1997) L208.
- [33] G. Liu, W. Lu, A model of concurrent lithium dendrite growth, SEI growth, SEI penetration and regrowth, J. Electrochem. Soc. 164 (2017) A1826–A1833.
- [34] D. Liu, Z. Shadike, R. Lin, K. Qian, H. Li, K. Li, S. Wang, Q. Yu, M. Liu, S. Ganapathy, X. Qin, Q.H. Yang, M. Wagemaker, F. Kang, X.Q. Yang, B. Li, Review of recent development of in situ/operando characterization techniques for lithium battery research, Adv. Mater. (2019) 1–57, 1806620.
- [35] P.P.R.M.L. Harks, F.M. Mulder, P.H.L. Notten, In situ methods for Li-ion battery research: a review of recent developments, J. Power Sources 288 (2015) 92–105.
- [36] M. Li, Z. Amirzadeh, R. De Marco, X.F. Tan, A. Whittaker, X. Huang, R. Wepf, R. Knibbe, In situ techniques for developing robust Li-S batteries, Small Methods 2 (2018) 1800133.
- [37] S.N.S. Hapuarachchi, Z. Sun, C. Yan, Li-ion batteries: advances in in situ techniques for characterization of failure mechanisms of Li-ion battery anodes (Adv. Sustainable Syst. 8-9/2018), Adv. Sustain. Syst. 2 (2018) 1870038.
- [38] K. Nishikawa, Y. Fukunaka, T. Sakka, Y.H. Ogata, J.R. Selman, Ionic mass transfer during electrochemical dissolution of Li metal in PC electrolyte solution, J. Electroanal. Chem. 584 (2005) 63–69.
- [39] K. Nishikawa, Y. Fukunaka, T. Sakka, Y.H. Ogata, J.R. Selman, Measurement of concentration profiles during electrodeposition of Li metal from LiP F6 -PC electrolyte solution, J. Electrochem. Soc. 154 (2007) 2–7.

- [40] M. Ota, S. Izuo, K. Nishikawa, Y. Fukunaka, E. Kusaka, R. Ishii, J.R. Selman, Measurement of concentration boundary layer thickness development during lithium electrodeposition onto a lithium metal cathode in propylene carbonate, J. Electroanal. Chem. 559 (2003) 175–183.
- [41] T. Nishida, K. Nishikawa, M. Rosso, Y. Fukunaka, Optical observation of Li dendrite growth in ionic liquid, Electrochim. Acta 100 (2013) 333–341.
- [42] K. Nishikawa, H. Naito, M. Kawase, T. Nishida, Morphological variation of electrodeposited Li in ionic liquid, ECS Trans 41 (2012) 3–10.
- [43] K. Nishikawa, T. Mori, T. Nishida, Y. Fukunaka, M. Rosso, T. Homma, In situ observation of dendrite growth of electrodeposited Li metal, J. Electrochem. Soc. 157 (2010) 1212–1217.
- [44] K. Nishikawa, T. Mori, T. Nishida, Y. Fukunaka, M. Rosso, Li dendrite growth and Li+ ionic mass transfer phenomenon, J. Electroanal. Chem. 661 (2011) 84–89.
- [45] P. Bai, J. Li, F.R. Brushett, M.Z. Bazant, Transition of lithium growth mechanisms in liquid electrolytes, Energy Environ. Sci. 9 (2016) 3221–3229.
- [46] J. Yamaki, S. Tobishima, K. Hayashi, Keiichi Saito, Y. Nemoto, M. Arakawa, A consideration of the morphology of electrochemically deposited lithium in an organic electrolyte, J. Power Sources 74 (1998) 219–227.
- [47] J. Steiger, D. Kramer, R. Mönig, Mechanisms of dendritic growth investigated by in situ light microscopy during electrodeposition and dissolution of lithium, J. Power Sources 261 (2014) 112–119.
- [48] J. Steiger, D. Kramer, R. Mönig, Microscopic observations of the formation, growth and shrinkage of lithium moss during electrodeposition and dissolution, Electrochim. Acta 136 (2014) 529–536.
- [49] O. Crowther, A.C. West, Effect of electrolyte composition on lithium dendrite growth, J. Electrochem. Soc. 155 (2008) 806–811.
- [50] J. Steiger, G. Richter, M. Wenk, D. Kramer, R. Mönig, Comparison of the growth of lithium filaments and dendrites under different conditions, Electrochem. Commun. 50 (2015) 11–14.
- [51] Z. Erlangung, Mechanisms of Dendrite Growth in Lithium Metal Batteries, Karlsruher Institut f
 ür Technologie (KIT), 2015.
- [52] F. Sagane, K.I. Ikeda, K. Okita, H. Sano, H. Sakaebe, Y. Iriyama, Effects of current densities on the lithium plating morphology at a lithium phosphorus oxynitride glass electrolyte/copper thin film interface, J. Power Sources 233 (2013) 34–42.
- [53] O. Crowther, A.C. West, Effect of electrolyte composition on lithium dendrite growth, J. Electrochem. Soc. 155 (2008) 806–811.
- [54] A. Pei, G. Zheng, F. Shi, Y. Li, Y. Cui, Nanoscale nucleation and growth of electrodeposited lithium metal, Nano Lett. 17 (2017) 1132–1139.
- [55] F. Sagane, K.I. Ikeda, K. Okita, H. Sano, H. Sakaebe, Y. Iriyama, Effects of current densities on the lithium plating morphology at a lithium phosphorus oxynitride glass electrolyte/copper thin film interface, J. Power Sources 233 (2013) 34–42.
- [56] L. Porz, T. Swamy, B.W. Sheldon, D. Rettenwander, T. Frömling, H.L. Thaman, S. Berendts, R. Uecker, W.C. Carter, Y.M. Chiang, Mechanism of lithium metal penetration through inorganic solid electrolytes, Adv. Energy Mater. 7 (2017) 1–12.
- [57] C. Monroe, J. Newman, The impact of elastic deformation on deposition kinetics at lithium/polymer interfaces, J. Electrochem. Soc. 152 (2005) A396.
- [58] A. Sharafi, H.M. Meyer, J. Nanda, J. Wolfenstine, J. Sakamoto, Characterizing the Li-Li7La3Zr2O12 interface stability and kinetics as a function of temperature and current density, J. Power Sources 302 (2016) 135–139.
- [59] L. Kong, Y. Xing, M.G. Pecht, In-situ observations of lithium dendrite growth, IEEE Access 6 (2018) 8387–8393.
- [60] M. Arakawa, S. ichi Tobishima, Y. Nemoto, M. Ichimura, J.ichi Yamaki, Lithium electrode cycleability and morphology dependence on current density, J. Power Sources 43 (1993) 27–35.
- [61] V. Stancovski, S. Badilescu, In situ Raman spectroscopic-electrochemical studies of lithium-ion battery materials: a historical overview, J. Appl. Electrochem. 44 (2014) 23-43
- [62] J.D. Forster, S.J. Harris, J.J. Urban, Mapping Li+ concentration and transport via in situ confocal Raman microscopy, J. Phys. Chem. Lett. 5 (2014) 2007–2011.
- [63] I. Rey, J.L. Bruneel, J. Grondin, L. Servant, J.C. Lassègues, Roman spectroelectrochemistry of a lithium/polymer electrolyte symmetric cell, J. Electrochem. Soc. 145 (1998) 3034–3042.
- [64] Q. Cheng, L. Wei, Z. Liu, N. Ni, Z. Sang, B. Zhu, W. Xu, M. Chen, Y. Miao, L. Q. Chen, W. Min, Y. Yang, Operando and three-dimensional visualization of anion depletion and lithium growth by stimulated Raman scattering microscopy, Nat. Commun. 9 (2018) 1–10.
- [65] Q. Cheng, L. Wei, Z. Liu, N. Ni, Z. Sang, B. Zhu, W. Xu, M. Chen, Y. Miao, L. Q. Chen, W. Min, Y. Yang, Operando and three-dimensional visualization of anion depletion and lithium growth by stimulated Raman scattering microscopy, Nat. Commun. 9 (2018) 1–10.
- [66] F. Orsini, A. Du Pasquier, B. Beaudoin, J. Tarascon, M. Trentin, N. Langenhuizen, E. De Beer, P. Notten, In situ Scanning Electron Microscopy (SEM) observation of interfaces within plastic lithium batteries, J. Power Sources 76 (1998) 19–29.
- [67] B.J. Neudecker, N.J. Dudney, J.B. Bates, 'Lithium-free' thin-film battery with in situ plated Li anode, J. Electrochem. Soc. 147 (2000) 517–523.
- [68] M. Nagao, A. Hayashi, M. Tatsumisago, T. Kanetsuku, T. Tsuda, S. Kuwabata, In situ SEM study of a lithium deposition and dissolution mechanism in a bulk-type solid-state cell with a Li2S-P2S5 solid electrolyte, Phys. Chem. Chem. Phys. 15 (2013) 18600–18606.
- [69] C.Y. Tang, S.J. Dillon, In situ scanning electron microscopy characterization of the mechanism for Li dendrite growth, J. Electrochem. Soc. 163 (2016) A1660–A1665.
- [70] M. Motoyama, M. Ejiri, Y. Iriyama, In-situ electron microscope observations of electrochemical Li deposition/dissolution with a LiPON electrolyte, Electrochemistry 82 (2014) 364–368.

- [71] S.H. Kim, K.H. Kim, H. Choi, D. Im, S. Heo, H.S. Choi, In situ observation of lithium metal plating in a sulfur-based solid electrolyte for all-solid-state batteries, J. Mater. Chem. A 7 (2019) 13650–13657.
- [72] A. Yulaev, V. Oleshko, P. Haney, J. Liu, Y. Qi, A.A. Talin, M.S. Leite, A. Kolmakov, From microparticles to nanowires and back: radical transformations in plated Li metal morphology revealed via in situ scanning electron microscopy, Nano Lett. 18 (2018) 1644–1650.
- [73] F. Sagane, R. Shimokawa, H. Sano, H. Sakaebe, Y. Iriyama, In-situ scanning electron microscopy observations of Li plating and stripping reactions at the lithium phosphorus oxynitride glass electrolyte/Cu interface, J. Power Sources 225 (2013) 245–250.
- [74] F. Sagane, R. Shimokawa, H. Sano, H. Sakaebe, Y. Iriyama, In-situ scanning electron microscopy observations of Li plating and stripping reactions at the lithium phosphorus oxynitride glass electrolyte/Cu interface, J. Power Sources 225 (2013) 245–250.
- [75] D. Lin, Y. Liu, Y. Li, Y. Li, A. Pei, J. Xie, W. Huang, Y. Cui, Fast galvanic lithium corrosion involving a Kirkendall-type mechanism Dingchang, Nat. Chem. 11 (2019) 382–389.
- [76] F. Han, A.S. Westover, J. Yue, X. Fan, F. Wang, M. Chi, D.N. Leonard, N. J. Dudney, H. Wang, C. Wang, High electronic conductivity as the origin of lithium dendrite formation within solid electrolytes, Nat. Energy 4 (2019) 187–196
- [77] T. Krauskopf, R. Dippel, H. Hartmann, K. Peppler, B. Mogwitz, F.H. Richter, W. G. Zeier, J. Janek, Lithium-metal growth kinetics on LLZO garnet-type solid electrolytes, Joule 3 (2019) 2030–2049.
- [78] G. Rong, X. Zhang, W. Zhao, Y. Qiu, M. Liu, F. Ye, Y. Xu, J. Chen, Y. Hou, W. Li, W. Duan, Y. Zhang, Liquid-phase electrochemical scanning electron microscopy for in situ investigation of lithium dendrite growth and dissolution, Adv. Mater. 29 (2017).
- [79] C. Fang, J. Li, M. Zhang, Y. Zhang, F. Yang, J.Z. Lee, M.-H. Lee, J. Alvarado, M. A. Schroeder, Y. Yang, B. Lu, N. Williams, M. Ceja, L. Yang, M. Cai, J. Gu, K. Xu, X. Wang, Y.S. Meng, Quantifying inactive lithium in lithium metal batteries, Nature 572 (2019) 511–515.
- [80] X.H. Liu, L. Zhong, L.Q. Zhang, A. Kushima, S.X. Mao, J. Li, Z.Z. Ye, J.P. Sullivan, J.Y. Huang, Lithium fiber growth on the anode in a nanowire lithium ion battery during charging, Appl. Phys. Lett. 98 (2011) 1–4.
- [81] H. Ghassemi, M. Au, N. Chen, P.A. Heiden, R.S. Yassar, Real-time observation of lithium fibers growth inside a nanoscale lithium-ion battery, Appl. Phys. Lett. 99 (2011) 1–4.
- [82] C. Ma, Y. Cheng, K. Yin, J. Luo, A. Sharafi, J. Sakamoto, J. Li, K.L. More, N. J. Dudney, M. Chi, Interfacial stability of Li metal-solid electrolyte elucidated via in situ electron microscopy, Nano Lett. 16 (2016) 7030–7036.
- [83] X. Tao, Y. Liu, W. Liu, G. Zhou, J. Zhao, D. Lin, C. Zu, O. Sheng, W. Zhang, H. W. Lee, Y. Cui, Solid-state lithium-sulfur batteries operated at 37 °C with composites of nanostructured Li7La3Zr2O12/carbon foam and polymer, Nano Lett. 17 (2017) 2967–2972.
- [84] Z. Zeng, W.I. Liang, H.G. Liao, H.L. Xin, Y.H. Chu, H. Zheng, Visualization of electrode-electrolyte interfaces in LiPF 6/EC/DEC electrolyte for lithium ion batteries via in situ TEM, Nano Lett. 14 (2014) 1745–1750.
- [85] R.L. Sacci, N.J. Dudney, K.L. More, L.R. Parent, I. Arslan, N.D. Browning, R. R. Unocic, Direct visualization of initial SEI morphology and growth kinetics during lithium deposition by in situ electrochemical transmission electron microscopy, Chem. Commun. 50 (2014) 2104–2107.
- [86] A. Kushima, K.P. So, C. Su, P. Bai, N. Kuriyama, T. Maebashi, Y. Fujiwara, M. Z. Bazant, J. Li, Liquid cell transmission electron microscopy observation of lithium metal growth and dissolution: root growth, dead lithium and lithium flotsams, Nano Energy 32 (2017) 271–279.
- [87] F.M. Ross, Electrochemical nucleation, growth and dendrite formation in liquid cell TEM, Microsc. Microanal. 16 (2010) 326–327.
- [88] E.R. White, S.B. Singer, V. Augustyn, W.A. Hubbard, M. Mecklenburg, B. Dunn, B. C. Regan, In situ transmission electron microscopy of lead dendrites and lead ions in aqueous solution, ACS Nano 6 (2012) 6308–6317.
- [89] B.L. Mehdi, J. Qian, E. Nasybulin, C. Park, D.A. Welch, R. Faller, H. Mehta, W. A. Henderson, W. Xu, C.M. Wang, J.E. Evans, J. Liu, J.G. Zhang, K.T. Mueller, N. D. Browning, Observation and quantification of nanoscale processes in lithium batteries by operando electrochemical (S)TEM, Nano Lett. 15 (2015) 2168–2173.
- [90] Z. Zhu, Y. Zhou, P. Yan, R.S. Vemuri, W. Xu, R. Zhao, X. Wang, S. Thevuthasan, D. R. Baer, C.M. Wang, In situ mass spectrometric determination of molecular structural evolution at the solid electrolyte interphase in lithium-ion batteries, Nano Lett. 15 (2015) 6170–6176.
- [91] A.J. Leenheer, K.L. Jungjohann, K.R. Zavadil, J.P. Sullivan, C.T. Harris, Lithium electrodeposition dynamics in aprotic electrolyte observed in situ via transmission electron Microscopy, ACS Nano 9 (2015) 4379–4389.
- [92] Y. He, X. Ren, Y. Xu, M.H. Engelhard, X. Li, J. Xiao, J. Liu, J. Zhang, W. Xu, C. Wang, Origin of lithium whisker formation and growth under stress, Nat. Nanotechnol. (2019), https://doi.org/10.1038/s41565-019-0558-z.
- [93] Y. Li, Y. Li, A. Pei, K. Yan, Y. Sun, C. Wu, L.-M. Joubert, R. Chin, A.L. Koh, Y. Yu, J. Perrino, B. Butz, S. Chu, Y. Cui, Atomic structure of sensitive battery materials and interfaces revealed by cryo electron microscopy, Science 358 (2017) 506–510 (80-.).
- [94] X. Wang, M. Zhang, J. Alvarado, S. Wang, M. Sina, B. Lu, J. Bouwer, W. Xu, J. Xiao, J.G. Zhang, J. Liu, Y.S. Meng, New insights on the structure of electrochemically deposited lithium metal and its solid electrolyte interphases via cryogenic TEM, Nano Lett. 17 (2017) 7606–7612.
- [95] X. Wang, Y. Li, Y.S. Meng, Cryogenic electron microscopy for characterizing and diagnosing batteries, Joule 2 (2018) 2225–2234.

- [96] M.J. Zachman, Z. Tu, S. Choudhury, L.A. Archer, L.F. Kourkoutis, Cryo-STEM mapping of solid–liquid interfaces and dendrites in lithium-metal batteries, Nature 560 (2018) 345–349.
- [97] K.A. Spoth, M.J. Zachman, D.A. Muller, L.F. Kourkoutis, Cryogenic STEM imaging and spectroscopy of electron beam sensitive materials, Microsc. Microanal. 25 (2019) 1660–1661.
- [98] W. Li, H. Yao, K. Yan, G. Zheng, Z. Liang, Y.M. Chiang, Y. Cui, The synergetic effect of lithium polysulfide and lithium nitrate to prevent lithium dendrite growth, Nat. Commun. 6 (2015).
- [99] J. Qian, W. Xu, P. Bhattacharya, M. Engelhard, W.A. Henderson, Y. Zhang, J. G. Zhang, Dendrite-free Li deposition using trace-amounts of water as an electrolyte additive, Nano Energy 15 (2015) 135–144.
- [100] Y. Xu, Y. He, H. Wu, W. Xu, C. Wang, Atomic structure of electrochemically deposited lithium metal and its solid electrolyte interphases revealed by cryo–electron microscopy, Microsc. Microanal. 25 (2019) 2220–2221.
- [101] Y. Liu, D. Lin, Y. Li, G. Chen, A. Pei, O. Nix, Y. Li, Y. Cui, Solubility-mediated sustained release enabling nitrate additive in carbonate electrolytes for stable lithium metal anode, Nat. Commun. 9 (2018) 1–10.
- [102] J. Wang, W. Huang, A. Pei, Y. Li, F. Shi, X. Yu, Y. Cui, Improving cyclability of Li metal batteries at elevated temperatures and its origin revealed by cryo-electron microscopy, Nat. Energy 4 (2019).
- [103] Y. Liu, D. Lin, Y. Li, G. Chen, A. Pei, O. Nix, Y. Li, Y. Cui, Solubility-mediated sustained release enabling nitrate additive in carbonate electrolytes for stable lithium metal anode, Nat. Commun. 9 (2018) 1–10.
- [104] J. Wang, W. Huang, A. Pei, Y. Li, F. Shi, X. Yu, Y. Cui, Improving cyclability of Li metal batteries at elevated temperatures and its origin revealed by cryo-electron microscopy, Nat. Energy 4 (2019).
- [105] Y. Li, W. Huang, Y. Li, A. Pei, D.T. Boyle, Y. Cui, Correlating structure and function of battery interphases at atomic resolution using cryoelectron microscopy, Joule 2 (2018) 2167–2177.
- [106] Y. Li, W. Huang, Y. Li, A. Pei, D.T. Boyle, Y. Cui, Correlating structure and function of battery interphases at atomic resolution using cryoelectron microscopy, Joule 2 (2018) 2167–2177.
- [107] I. Yoon, S. Jurng, D.P. Abraham, B.L. Lucht, P.R. Guduru, Measurement of mechanical and fracture properties of solid electrolyte interaphase on lithium metal anodes in lithium ion batteries, Energy Storage Mater. (2019), https://doi. org/10.1016/j.ensm.2019.10.009.
- [108] M. Kitta, H. Sano, Real-time observation of Li deposition on a Li electrode with operand atomic force microscopy and surface mechanical imaging, Langmuir 33 (2017) 1861–1866.
- [109] Y.S. Cohen, Y. Cohen, D. Aurbach, Micromorphological studies of lithium electrodes in alkyl carbonate solutions using in situ atomic force microscopy, J. Phys. Chem. B 104 (2000) 12282–12291.
- [110] I. Yoon, S. Jurng, D.P. Abraham, B.L. Lucht, P.R. Guduru, In situ measurement of the plane-strain modulus of the solid electrolyte interphase on lithium-metal anodes in ionic liquid electrolytes, Nano Lett. 18 (2018) 5752–5759.
- [111] I. Yoon, S. Jurng, D.P. Abraham, B.L. Lucht, P.R. Guduru, Measurement of mechanical and fracture properties of solid electrolyte interaphase on lithium metal anodes in lithium ion batteries, Energy Storage Mater. (2019), https://doi. org/10.1016/j.ensm.2019.10.009.
- [112] R. Mogi, M. Inaba, S.K. Jeong, Y. Iriyama, T. Abe, Z. Ogumi, Effects of some organic additives on lithium deposition in propylene carbonate, J. Electrochem. Soc. 149 (2002) 1578–1583.
- [113] C. Shen, G. Hu, L.-Z. Cheong, S. Huang, J.-G. Zhang, D. Wang, Direct observation of the growth of lithium dendrites on graphite anodes by operando EC-AFM, Small Methods 2 (2018) 1700298.
- [114] B. Liu, W. Xu, J. Tao, P. Yan, J. Zheng, M.H. Engelhard, D. Lu, C. Wang, J. G. Zhang, Enhanced cyclability of lithium—oxygen batteries with electrodes protected by surface films induced via in situ electrochemical process, Adv. Energy Mater. 8 (2018).
- [115] N.W. Li, Y. Shi, Y.X. Yin, X.X. Zeng, J.Y. Li, C.J. Li, L.J. Wan, R. Wen, Y.G. Guo, A flexible solid electrolyte interphase layer for long-life lithium metal anodes, Angew. Chem. Int. Ed. 57 (2018) 1505–1509.
- [116] C. Campbell, Y.M. Lee, K.Y. Cho, Y.G. Lee, B. Lee, C. Phatak, S. Hong, Effect of nanopatterning on mechanical properties of Lithium anode, Sci. Rep. 8 (2018) 1–9.
- [117] O.O. Taiwo, 3D and 4D Characterisation of Lithium Ion Battery Electrode Microstructures Using X-Ray Tomography, 2016, p. 219.
- [118] Y. Wu, N. Liu, Visualizing battery reactions and processes by using in situ and in operando microscopies, Chem 4 (2018) 438–465.
- [119] P.R. Shearing, Y. Wu, S.J. Harris, N. Brandon, In situ X-ray spectroscopy and imaging of battery materials, Electrochem. Soc. Interfaces 457 (2011) 43–47.
- [120] D. Schröder, C.L. Bender, T. Arlt, M. Osenberg, A. Hilger, S. Risse, M. Ballauff, I. Manke, J. Janek, In operando x-ray tomography for next-generation batteries: a systematic approach to monitor reaction product distribution and transport processes, J. Phys. D Appl. Phys. 49 (2016).
- [121] K.J. Harry, D.T. Hallinan, D.Y. Parkinson, A. a Macdowell, N.P. Balsara, Detection of subsurface structures underneath dendrites formed on cycled lithium metal electrodes, Nat. Mater. 13 (2013) 69–73.
- [122] D.S. Eastwood, P.M. Bayley, H.J. Chang, O.O. Taiwo, J. Vila-Comamala, D.J. L. Brett, C. Rau, P.J. Withers, P.R. Shearing, C.P. Grey, P.D. Lee, Three-dimensional characterization of electrodeposited lithium microstructures using synchrotron X-ray phase contrast imaging, Chem. Commun. 51 (2015) 266–268.
- [123] O.O. Taiwo, D.P. Finegan, J.M. Paz-Garcia, D.S. Eastwood, A.J. Bodey, C. Rau, S. A. Hall, D.J.L. Brett, P.D. Lee, P.R. Shearing, Investigating the evolving

- microstructure of lithium metal electrodes in 3D using X-ray computed tomography, Phys. Chem. Chem. Phys. 19 (2017) 22111–22120.
- [124] F. Sun, L. Zielke, H. Markötter, A. Hilger, D. Zhou, R. Moroni, R. Zengerle, S. Thiele, J. Banhart, I. Manke, Morphological evolution of electrochemically plated/stripped lithium microstructures investigated by synchrotron X-ray phase contrast tomography, ACS Nano 10 (2016) 7990–7997.
- [125] F. Sun, R. Moroni, K. Dong, H. Markötter, D. Zhou, A. Hilger, L. Zielke, R. Zengerle, S. Thiele, J. Banhart, I. Manke, Study of the mechanisms of internal short circuit in a Li/Li cell by synchrotron X-ray phase contrast tomography, ACS Energy Lett. 2 (2017) 94–104.
- [126] J.H. Cheng, A.A. Assegie, C.J. Huang, M.H. Lin, A.M. Tripathi, C.C. Wang, M. T. Tang, Y.F. Song, W.N. Su, B.J. Hwang, Visualization of lithium plating and stripping via in operando transmission X-ray microscopy, J. Phys. Chem. C 121 (2017) 7761–7766.
- [127] J. Cheng, A.A. Assegie, C. Huang, M. Lin, A.M. Tripathi, C. Wang, M. Tang, Y. Song, W. Su, B.J. Hwang, Visualization of Lithium Plating and Stripping via in Operando Transmission X - Ray Microscopy, 2017, https://doi.org/10.1021/acs. jpcc.7b01414.
- [128] S. Frisco, D.X. Liu, A. Kumar, J.F. Whitacre, C.T. Love, K.E. Swider-Lyons, S. Litster, Internal morphologies of cycled Li-metal electrodes investigated by nano-scale resolution X-ray computed tomography, ACS Appl. Mater. Interfaces 9 (2017) 18748–18757.
- [129] J. Kasemchainan, S. Zekoll, D. Spencer Jolly, Z. Ning, G.O. Hartley, T.J. Marrow, P.G. Bruce, Critical stripping current leads to dendrite formation on plating in 3 lithium anode solid electrolyte cells, Nat. Mater. (2019), https://doi.org/ 10.1038/s41563-019-0438-9.
- [130] J. Kasemchainan, S. Zekoll, D. Spencer Jolly, Z. Ning, G.O. Hartley, J. Marrow, P. G. Bruce, Critical stripping current leads to dendrite formation on plating in lithium anode solid electrolyte cells, Nat. Mater. 18 (2019) 1105–1111.
- [131] F. Sun, X. He, X. Jiang, M. Osenberg, J. Li, D. Zhou, K. Dong, A. Hilger, X. Zhu, R. Gao, X. Liu, K. Huang, D. Ning, H. Markötter, L. Zhang, F. Wilde, Y. Cao, M. Winter, I. Manke, Advancing knowledge of electrochemically generated lithium microstructure and performance decay of lithium ion battery by synchrotron X-ray tomography, Mater. Today 27 (2018) 21–32.
- [132] F. Shen, M.B. Dixit, X. Xiao, K.B. Hatzell, Effect of pore connectivity on Li dendrite propagation within LLZO electrolytes observed with synchrotron X-ray tomography, ACS Energy Lett. 3 (2018) 1056–1061.
- [133] H. Wang, R.G. Downing, J.A. Dura, D.S. Hussey, In situ neutron techniques for studying lithium ion batteries, ACS (Am. Chem. Soc.) Symp. Ser. (2012), https:// doi.org/10.1021/bk-2012-1096.ch006.
- [134] X. Zhang, T.W. Verhallen, F. Labohm, M. Wagemaker, Direct observation of Li-ion transport in electrodes under nonequilibrium conditions using neutron depth profiling, Adv. Energy Mater. 5 (2015) 1–8.
- [135] J.F.M. Oudenhoven, F. Labohm, M. Mulder, R.A.H. Niessen, F.M. Mulder, P.H. L. Notten, In situ neutron depth profiling: a powerful method to probe lithium transport in micro-batteries, Adv. Mater. 23 (2011) 4103–4106.
- [136] S. Lv, T. Verhallen, A. Vasileiadis, F. Ooms, Y. Xu, Z. Li, Z. Li, M. Wagemaker, Operando monitoring the lithium spatial distribution of lithium metal anodes, Nat. Commun. 9 (2018) 1–12.
- [137] V. Zinth, C. Von Lüders, M. Hofmann, J. Hattendorff, I. Buchberger, S. Erhard, J. Rebelo-Kornmeier, A. Jossen, R. Gilles, Lithium plating in lithium-ion batteries at sub-ambient temperatures investigated by in situ neutron diffraction, J. Power Sources 271 (2014) 152–159.
- [138] C. Wang, Y. Gong, J. Dai, L. Zhang, H. Xie, G. Pastel, B. Liu, E. Wachsman, H. Wang, L. Hu, In situ neutron depth profiling of lithium metal-garnet interfaces for solid state batteries, J. Am. Chem. Soc. 139 (2017) 14257–14264.
- [139] Q. Li, T. Yi, X. Wang, H. Pan, B. Quan, T. Liang, X. Guo, X. Yu, H. Wang, X. Huang, L. Chen, H. Li, In-situ visualization of lithium plating in all-solid-state lithiummetal battery, Nano Energy 63 (2019) 103895.
- [140] B. Song, I. Dhiman, J.C. Carothers, G.M. Veith, J. Liu, H.Z. Bilheux, A. Huq, Dynamic lithium distribution upon dendrite growth and shorting revealed by operando neutron imaging, ACS Energy Lett. (2019) 2402–2408, https://doi.org/ 10.1021/acsenergylett.9b01652.
- [141] S. Lv, T. Verhallen, A. Vasileiadis, F. Ooms, Y. Xu, Z. Li, Z. Li, M. Wagemaker, Operando monitoring the lithium spatial distribution of lithium metal anodes, Nat. Commun. 9 (2018) 1–12.
- [142] C. von Lüders, V. Zinth, S.V. Erhard, P.J. Osswald, M. Hofmann, R. Gilles, A. Jossen, Lithium plating in lithium-ion batteries investigated by voltage relaxation and in situ neutron diffraction, J. Power Sources 342 (2017) 17–23.
- [143] F. Han, A.S. Westover, J. Yue, X. Fan, F. Wang, M. Chi, D.N. Leonard, N. J. Dudney, H. Wang, C. Wang, High electronic conductivity as the origin of lithium dendrite formation within solid electrolytes, Nat. Energy 4 (2019) 187–196.
- [144] Q. Li, T. Yi, X. Wang, H. Pan, B. Quan, T. Liang, X. Guo, X. Yu, H. Wang, X. Huang, L. Chen, H. Li, In-situ visualization of lithium plating in all-solid-state lithiummetal battery, Nano Energy 63 (2019) 103895.
- [145] Y. Song, L. Yang, W. Zhao, Z. Wang, Y. Zhao, Z. Wang, Q. Zhao, H. Liu, F. Pan, Revealing the short-circuiting mechanism of garnet-based solid-state electrolyte, Adv. Energy Mater. 9 (2019) 1–6.
- [146] A.M. Tripathi, W.-N. Su, B. Hwang, J. In situ analytical techniques for battery interface analysis, Chem. Soc. Rev. 47 (2018) 736–851.
- [147] R.K. Harris, E.D. Becker, S.M. Cabral De Menezes, P. Granger, R.E. Hoffman, K. W. Zilm, Further conventions for NMR shielding and chemical shifts IUPAC recommendations 2008, Solid State Nucl. Magn. Reson. 33 (2008) 41–56.
- [148] M. Klett, M. Giesecke, A. Nyman, F. Hallberg, R.W. Lindström, G. Lindbergh, I. Furó, Quantifying mass transport during polarization in a Li Ion battery

- electrolyte by in situ 7Li NMR imaging, J. Am. Chem. Soc. 134 (2012)
- [149] J. Arai, R. Nakahigashi, Study of Li metal deposition in lithium ion battery during low-temperature cycle using in situ solid-state 7Li nuclear magnetic resonance, J. Electrochem. Soc. 164 (2017) A3403–A3409.
- [150] O. Pecher, J. Carretero-Gonzalez, K.J. Griffith, C.P. Grey, Materials' methods: NMR in battery research, Chem. Mater. 29 (2017) 213–242.
- [151] D.M. Itkis, J.J. Velasco-Velez, A. Knop-Gericke, A. Vyalikh, M.V. Avdeev, L. V. Yashina, Probing operating electrochemical interfaces by photons and neutrons, ChemElectroChem 2 (2015) 1427–1445.
- [152] S. Klamor, K. Zick, T. Oerther, F.M. Schappacher, M. Winter, G. Brunklaus, 7Li in situ 1D NMR imaging of a lithium ion battery, Phys. Chem. Chem. Phys. 17 (2015) 4458–4465.
- [153] P. Verma, P. Maire, P. Novák, Electrochimica Acta Review article A review of the features and analyses of the solid electrolyte interphase in Li-ion batteries, Electrochim. Acta 55 (2010) 6332–6341.
- [154] M. Leskes, G. Kim, T. Liu, A.L. Michan, F. Aussenac, P. Dorffer, S. Paul, C.P. Grey, Surface-sensitive NMR detection of the solid electrolyte interphase layer on reduced graphene oxide, J. Phys. Chem. Lett. 8 (2017) 1078–1085.
- [155] M.A. Hope, B.L.D. Rinkel, A.B. Gunnarsdóttir, K. Märker, S. Paul, C.P. Grey, DNP-enhanced NMR of lithium Dendrites: selective observation of the solid electrolyte interphase, ChemRxiv (2019) 1–33.
- [156] S. Chandrashekar, N.M. Trease, H.J. Chang, L.S. Du, C.P. Grey, A. Jerschow, 7Li MRI of Li batteries reveals location of microstructural lithium, Nat. Mater. 11 (2012) 311–315.
- [157] H.J. Chang, A.J. Ilott, N.M. Trease, M. Mohammadi, A. Jerschow, C.P. Grey, Correlating microstructural lithium metal growth with electrolyte salt depletion in lithium batteries Using7Li MRI, J. Am. Chem. Soc. 137 (2015) 15209–15216.
- [158] A.J. Ilott, M. Mohammadi, H.J. Chang, C.P. Grey, A. Jerschow, Real-time 3D imaging of microstructure growth in battery cells using indirect MRI, Proc. Natl. Acad. Sci. U.S.A. 113 (2016) 10779–10784.
- [159] M. Mohammadi, A. Jerschow, In situ and operando magnetic resonance imaging of electrochemical cells: a perspective, J. Magn. Reson. 308 (2019) 106600.
- [160] P.H. Chien, X. Feng, M. Tang, J.T. Rosenberg, S. O'Neill, J. Zheng, S.C. Grant, Y. Y. Hu, Li distribution heterogeneity in solid electrolyte Li10GeP2S12 upon electrochemical cycling probed by 7Li MRI, J. Phys. Chem. Lett. 9 (2018) 1990–1998.
- [161] L.E. Marbella, S. Zekoll, J. Kasemchainan, S.P. Emge, P.G. Bruce, C.P. Grey, 7 Li NMR chemical shift imaging to detect microstructural growth of lithium in allsolid-state batteries. Chem. Mater. 31 (2019) 2762–2769.
- [162] A.J. Ilott, M. Mohammadi, C.M. Schauerman, M.J. Ganter, A. Jerschow, Rechargeable lithium-ion cell state of charge and defect detection by in-situ inside-out magnetic resonance imaging, Nat. Commun. 9 (2018) 1–7.
- [163] J. Wandt, C. Marino, H.A. Gasteiger, P. Jakes, R.A. Eichel, J. Granwehr, Operando electron paramagnetic resonance spectroscopy-formation of mossy lithium on lithium anodes during charge-discharge cycling, Energy Environ. Sci. 8 (2015) 1358–1367.
- [164] A. Niemöller, P. Jakes, R.A. Eichel, J. Granwehr, EPR imaging of metallic lithium and its application to dendrite localisation in battery separators, Sci. Rep. 8 (2018) 1–7.

- [165] F.J. Dyson, Electron spin resonance absorption in metals. II. Theory of electron diffusion and the skin effect, Phys. Rev. 98 (1955) 349–359.
- [166] G. Feher, A.F. Kip, Electron spin resonance absorption in metals. I. Experimental, Phys. Rev. 98 (1955) 337–348.
- [167] M. Sathiya, J. Leriche, E. Salager, D. Gourier, J. Tarascon, H. Vezin, Electron paramagnetic resonance imaging for real-time monitoring of Li-ion batteries, Nat. Commun. (2015) 1–7, https://doi.org/10.1038/ncomms7276.
- [168] C. Szczuka, A. Niemöller, P. Jakes, J. Granwehr, Application of bruker EMXnano for in operando analysis of metallic lithium microstructure, Bruker Rep. 7 (2018) 1–5.
- [169] G. McMullan, A.R. Faruqi, R. Henderson, Direct electron detectors, in: Methods in Enzymology, vol. 579, Elsevier Inc., 2016.
- [170] V. Yurkiv, T. Foroozan, A. Ramasubramanian, R. Shahbazian-Yassar, F. Mashayek, Phase-field modeling of solid electrolyte interface (SEI) influence on Li dendritic behavior, Electrochim. Acta 265 (2018) 609–619.
- [171] A. Ramasubramanian, V. Yurkiv, T. Foroozan, M. Ragone, R. Shahbazian-Yassar, F. Mashayek, Lithium diffusion mechanism through solid-electrolyte interphase in rechargeable lithium batteries, J. Phys. Chem. C 123 (2019) 10237–10245.
- [172] M.L. Taheri, E.A. Stach, I. Arslan, P.A. Crozier, B.C. Kabius, T. LaGrange, A. M. Minor, S. Takeda, M. Tanase, J.B. Wagner, R. Sharma, Current status and future directions for in situ transmission electron microscopy, Ultramicroscopy 170 (2016) 86–95.
- [173] K. Yan, H.W. Lee, T. Gao, G. Zheng, H. Yao, H. Wang, Z. Lu, Y. Zhou, Z. Liang, Z. Liu, S. Chu, Y. Cui, K. Yan, H.W. Lee, T. Gao, G. Zheng, H. Yao, H. Wang, Z. Lu, Y. Zhou, Z. Liang, Z. Liu, S. Chu, Y. Cui, Ultrathin two-dimensional atomic crystals as stable interfacial layer for improvement of lithium metal anode, Nano Lett. 14 (2014) 6016–6022.
- [174] Q. Li, S. Tan, L. Li, Y. Lu, Y. He, Understanding the molecular mechanism of pulse current charging for stable lithium-metal batteries, Sci. Adv. 3 (2017) 1–10.
- [175] L. Li, S. Basu, Y. Wang, Z. Chen, P. Hundekar, B. Wang, J. Shi, Y. Shi, S. Narayanan, N. Koratkar, Self-heating-induced healing of lithium dendrites, Science 359 (2018) 1513–1516 (80-.).
- [176] X.B. Cheng, T.Z. Hou, R. Zhang, H.J. Peng, C.Z. Zhao, J.Q. Huang, Q. Zhang, Dendrite-free lithium deposition induced by uniformly distributed lithium ions for efficient lithium metal batteries, Adv. Mater. 28 (2016) 2888–2895.
- [177] F. Pei, A. Fu, W. Ye, J. Peng, X. Fang, M.S. Wang, N. Zheng, Robust lithium metal anodes realized by lithiophilic 3D porous current collectors for constructing highenergy lithium-sulfur batteries, ACS Nano 13 (2019) 8337–8346.
- [178] O. Crowther, A.C. West, Effect of electrolyte composition on lithium dendrite growth, J. Electrochem. Soc. 155 (2008) A806.
- [179] B.L. Mehdi, A. Stevens, J. Qian, C. Park, W. Xu, W.A. Henderson, J.G. Zhang, K. T. Mueller, N.D. Browning, The impact of Li grain size on coulombic efficiency in Li batteries, Sci. Rep. 6 (2016) 1–8.
- [180] H. Wang, Y.Y. Li, Y.Y. Li, Y. Liu, D. Lin, C. Zhu, G. Chen, A. Yang, K. Yan, H. Chen, Y. Zhu, J. Li, J. Xie, J. Xu, Z. Zhang, R. Vilá, A. Pei, K. Wang, Y. Cui, Wrinkled graphene cages as hosts for high-capacity Li metal anodes shown by cryogenic electron microscopy, Nano Lett. (2019), https://doi.org/10.1021/acs.nanolett.8bi04906